Structural Safety 111 (2024) 102498

Contents lists available at ScienceDirect

Structural Safety

journal homepage: www.elsevier.com/locate/strusafe

A reduced-order model approach for fuzzy fields analysis

Nataly A. Manque [a,*], Marcos A. Valdebenito [a], Pierre Beaurepaire [b], David Moens [c], Matthias G.R. Faes [a]

[a] Chair for Reliability Engineering, TU Dortmund University, Leonhard-Euler-Str. 5, Dortmund 44227, Germany
[b] Université Clermont Auvergne, CNRS, SIGMA Clermont, Institut Pascal, F-63000 Clermont-Ferrand, France
[c] Department of Mechanical Engineering - LMSD Division, KU Leuven, Jan De Nayerlaan 5, 2860 St.-Katelijne-Waver, Belgium

ARTICLE INFO

Keywords:
Fuzzy fields
Reduced-order model
Spatial uncertainty
Heat transfer
Seepage analysis

ABSTRACT

Characterization of the response of systems with governing parameters that exhibit both uncertainties and spatial dependencies can become quite challenging. In these cases, the accuracy of conventional probabilistic methods to quantify the uncertainty may be strongly affected by the availability of data. In such a scenario, fuzzy fields become an efficient tool for solving problems that exhibit uncertainty with a spatial component. Nevertheless, the propagation of the uncertainty associated with input parameters characterized as fuzzy fields towards the output response of a model can be quite demanding from a numerical point of view. Therefore, this paper proposes an efficient numerical strategy for forward uncertainty quantification under fuzzy fields. This strategy is geared towards the analysis of steady-state, linear systems. To reduce the numerical cost associated with uncertainty propagation, full system analyses are replaced by a reduced-order model. This reduced-order model projects the equilibrium equations into a small-dimensional space constructed from a single analysis of the system plus sensitivity analysis. The associated basis is enriched to ensure the quality of the approximate response and numerical cost reduction. Case studies of heat transfer and seepage analysis show that with the presented strategy, it is possible to accurately estimate the fuzzy responses with reduced numerical effort.

1. Introduction

The presence of spatial uncertainty is ubiquitous to almost all practical engineering problems and is a major challenge for the design of robust systems [1,2]. Spatial uncertainty arises from measurement errors, limitations in data collection methods, and inaccuracies in spatial representations, and thus refers to the lack of knowledge or precision about the exact values of a property or phenomenon of a system in space [3]. These uncertainties are traditionally incorporated into numerical models using probability theory, such as the well-known random field method [4]. Nonetheless, when dealing with spatial uncertainties, challenges such as data sparseness are even more pronounced than for properties that are not affected by the spatial component. Typically, there is limited and incomplete spatial data about the system under study. As a result, such information is sometimes insufficient to construct a robust probabilistic model of the uncertain parameters [5–7]. To address these problems, set-based methods have been developed in recent years [8,9]. Within this group, one can find, fuzzy analysis [10,11], imprecise probabilities [7,12], and interval methods [13–17].

Among these techniques, interval fields [18] have proven to be particularly practical when dealing with limited information. In this approach, uncertainty is quantified by establishing intervals (defined by lower and upper bounds) at specific locations, called control points, where the goal is to quantify extreme values of the properties of the system [19]. Here, spatial dependencies are modeled by an expansion of basis functions weighted by the interval-valued scalars at these locations. Thus, the uncertainty present in the system is encapsulated to that present at the locations where the control points are defined [20]. Nevertheless, the definition of intervals to encapsulate the uncertainty around control points can sometimes be overly strict (and conservative). In addition, users typically have an interest in assessing the sensitivity of the response. For these reasons, the concept of fuzzy fields [21,22] emerges, moving from the use of intervals at control points to the characterization of uncertainty by membership functions. This integration of fuzziness serves to provide the users with a greater degree of flexibility in the analysis. As a result, it allows the study of different scenarios, giving them more information to produce robust designs [23].

The main challenge addressed in this work is to propagate uncertainty associated with fuzzy fields in an efficient way. The class of problems considered corresponds to the analysis of linear systems

* Corresponding author.
E-mail address: nataly.manque@tu-dortmund.de (N.A. Manque).

https://doi.org/10.1016/j.strusafe.2024.102498
Received 22 January 2024; Received in revised form 13 May 2024; Accepted 20 June 2024
Available online 25 June 2024

Nomenclature

Symbol	Description
α	Membership level
α_l	lth membership level
$\boldsymbol{\beta}$	Vector whose components depend on the uncertain parameters
ξ	Uncertain parameter
ξ_j	Uncertain parameter at control point j
ξ_α^I	Interval associated with the membership level α
$\xi_\alpha^I(\boldsymbol{x})$	Interval field associated with the membership level α
$\xi_{j,\alpha}^I$	Interval associated with the membership level α at the jth control point
$\underline{\xi}_\alpha$	Lower bound of interval ξ_α^I
$\bar{\xi}_\alpha$	Upper bound of interval ξ_α^I
$\boldsymbol{\xi}$	Vector of uncertain parameters
$\boldsymbol{\xi}^0$	Expansion point to construct the reduced basis
$\boldsymbol{\xi}^*$	Realization of the uncertain parameters
$\hat{\xi}$	Fuzzy variable
$\hat{\xi}_j$	Fuzzy variable at the jth control point
$\hat{\xi}(\boldsymbol{x})$	Fuzzy field
Ξ	Fundamental set
$\boldsymbol{\gamma}$	Vector of constant coefficients to compute the response of interest
$\boldsymbol{\Phi}$	Reduced basis
$\boldsymbol{\Phi}_0$	Initial reduced basis
$\boldsymbol{\Phi}_1$	First updated reduced basis
$\boldsymbol{\phi}_i$	ith component vector of the reduced basis
$\psi(\cdot,\cdot)$	Basis function
$d(\cdot,\cdot)$	Distance measure
$e(\cdot)$	Error associated with the reduced-order model
$\boldsymbol{f}$	External loads vector
$\boldsymbol{f}_R$	External loads vector of the reduced system
$\boldsymbol{K}$	System's matrix
$\boldsymbol{K}_k$	System's matrices not affected by the uncertainty
$\boldsymbol{K}_R$	System's matrix of the reduced system
n_ξ	Number of uncertain parameters
n_b	Number of control points
n_c	Number of discrete levels to approximate the membership function
n_d	Number of degrees-of-freedom
n_e	Number of finite elements
n_r	Number of vectors of the reduced basis
p	Power of the distance measure
r	Response of the system
r^A	Approximate response of the system
$r_{\alpha_l}^I$	Interval response for membership level α_l
$\underline{r}_{\alpha_l}$	Lower bound of response for membership level α_l
$\bar{r}_{\alpha_l}$	Upper bound of response for membership level α_l
$\underline{r}_{\alpha_l}^A$	Lower bound of approximate response for membership level α_l
$\bar{r}_{\alpha_l}^A$	Upper bound of approximate response for membership level α_l
$\boldsymbol{u}$	Response vector of the system
$\boldsymbol{u}^A$	Approximate response vector of the system
$\boldsymbol{v}(\cdot)$	Projection of the response over the reduced basis
$w(\cdot,\cdot)$	Weight function
$\boldsymbol{x}$	Spatial coordinate
$\boldsymbol{x}_j$	Coordinates of the jth control point
$\boldsymbol{x}_{C,q}$	Coordinates of the centroid of the qth element
$\boldsymbol{X}$	Matrix of coordinates of the control points

under static external action. Uncertainty propagation from the input parameters to the response is not a straightforward task when using fuzzy fields to capture spatial uncertainty. Repeated deterministic analysis of the system must be performed for different realizations of the input parameters to obtain the fuzzy response [24]. Therefore, the objective is to reduced the numerical cost associated with the estimation of the fuzzy response. In order to effectively deal with this difficulty, a surrogate model [25] corresponding to a reduced-order

model is considered to replace the original finite element model [26]. The advantage of this surrogate model lies in its ability to map the system equations onto a lower dimensional basis, which significantly reduces the time required to compute the response. This reduced basis is particularly suitable because its construction requires only one exact analysis, which includes the effect of each uncertain parameter through a sensitivity analysis [27]. For this sensitivity analysis, the first derivatives of the system response with respect to the uncertain parameters are calculated. In this work, the ortho-normalization of the reduced basis is performed via Gram–Schmidt process [28]. An updating strategy of the reduced basis is proposed to guarantee the accuracy of the approximation. For this purpose, the error associated with the reduced basis is monitored as the uncertainty propagates, and the basis is enriched if necessary to keep the error below a certain threshold.

Consequently, the novelty of this work primarily resides in the creation of a surrogate model, which utilizes a reduced basis for performing analysis with fuzzy fields that is updated on-the-fly. Initially, the construction of the reduced basis necessitates only an exact analysis. By integrating sensitivity analysis into the process of basis construction, a balance between computational efficiency and precision is achieved. Subsequently, the reduced basis is updated efficiently based on the error encountered while determining the response bounds. Specifically, the proposal is to monitor solely the error associated with the optimal response bounds. This approach enhances the quality of the approximation without sacrificing numerical efficiency.

This paper is organized as follows. Section 2 presents the class of systems considered in this work and the fuzzy field formulation for characterizing uncertain parameters with spatial dependencies of a system. It also explains the process of forward uncertainty propagation for quantifying the uncertainty associated with the system response. Section 3 presents the approach used to reduce the computational effort required to compute the fuzzy response. It discusses the construction of the reduced basis, the error monitoring strategy, and the technique for updating the reduced basis. The implementation of the proposed technique is illustrated and discussed in Section 4 using an example of heat transfer on a concrete block made with by-products and seepage under an impervious dam. Conclusions are drawn in Section 5.

2. Formulation of the problem

2.1. Governing equations

Consider a steady-state, linear system whose behavior is modeled with the finite element method. It is assumed that the values of the parameters involved in the model (e.g. material properties) cannot be precisely determined due to problems such as lack of knowledge, imprecision, vagueness and scarcity of data. Therefore, the input parameters are affected by epistemic uncertainty. These parameters are collected in a vector $\boldsymbol{\xi}$ of dimension n_{ξ}. Under the action of static actions, the equilibrium equation of the system is,

$$\boldsymbol{K}(\boldsymbol{\xi})\,\boldsymbol{u}(\boldsymbol{\xi}) = \boldsymbol{f}(\boldsymbol{\xi}) \tag{1}$$

where $\boldsymbol{K}(\boldsymbol{\xi})$ is the system's matrix of dimension $n_d \times n_d$, $\boldsymbol{f}(\boldsymbol{\xi})$ is the vector associated with the external loads, whose dimension is n_d, and $\boldsymbol{u}(\boldsymbol{\xi})$ is the response vector of dimension n_d. It is assumed that $\boldsymbol{K}(\boldsymbol{\xi})$ is positive-definite and $\boldsymbol{f}(\boldsymbol{\xi}) \neq 0$. It is observed that the system's matrix $\boldsymbol{K}(\boldsymbol{\xi})$ and the external loads $\boldsymbol{f}(\boldsymbol{\xi})$ depend on the uncertain input variables $\boldsymbol{\xi}$. Therefore, the response of the system $\boldsymbol{u}(\boldsymbol{\xi})$ also depends on these uncertain input parameters. Note that the number of degrees-of-freedom n_d needed to represent the system using the finite element (FE) method is usually large. Therefore, the solution of Eq. (1) requires a considerable numerical effort. Furthermore, it should be noted that Eq. (1) allows the analysis of various steady-state physical phenomena [29], including for example heat transfer [30,31] and seepage analysis [13,32].

It is considered that the system's matrix $\boldsymbol{K}(\boldsymbol{\xi})$ admits the following parametric representation:

$$\boldsymbol{K}(\boldsymbol{\xi}) = \boldsymbol{K}_0 + \sum_{k=1}^{n_{\xi}} \boldsymbol{K}_k \xi_k \tag{2}$$

where, $\boldsymbol{K}_k$, $k = 1, \ldots, n_{\xi}$ are matrices of dimension $n_d \times n_d$ that are unaffected by the uncertainty; and ξ_k is the kth component of vector $\boldsymbol{\xi}$.

In practice, designers are usually interested in finding out a particular response of the system $r(\boldsymbol{\xi})$, which is assumed to be given by:

$$r(\boldsymbol{\xi}) = \boldsymbol{\gamma}^T \boldsymbol{u}(\boldsymbol{\xi}) \tag{3}$$

where $\boldsymbol{\gamma}$ is a vector of constant coefficients of dimension n_d and $(\cdot)^T$ denotes the transpose of the argument. In this paper, it is assumed that the response of interest is a scalar. Nevertheless, the definition presented in Eq. (3) can be extended to consider several responses of interest. Furthermore, for more complex responses, the parameter $\boldsymbol{\gamma}$ can be considered as an operator that allows post-processing of the solution $\boldsymbol{u}(\boldsymbol{\xi})$.

2.2. Fuzzy variables

Following a set-based approach, the definition of intervals is a straightforward way to describe the uncertainty of the input parameters collected in the vector $\boldsymbol{\xi}$ [6]. For this purpose, a lower and an upper bound are used to define each uncertain parameter. Nevertheless, in cases where it is necessary to relax the precise identification of these bounds, fuzzy set theory [33] provides a useful framework for achieving this goal [34]. Fuzzy set theory allows the incorporation of uncertainty through linguistic descriptions [35]. It is therefore well-suited to situations where the available data is limited or stems from expert elicitations. In this context, the uncertain parameters can be characterized as fuzzy variables by means of membership functions.

For the sake of simplicity, consider that there is a single uncertain parameter ξ in the linear system of Eq. (1). This uncertain parameter ξ is characterized as a fuzzy variable $\hat{\xi}$, which comprises the fundamental set Ξ, which corresponds to all physical values that ξ can take, and the membership function $\mu_{\hat{\xi}}$, which describes the degree of belongingness of these values. This membership function is such that $\mu_{\hat{\xi}}(\xi) \in [0, 1]$. Note that in classical set theory, the membership function $\mu_{\hat{\xi}}(\xi)$ is equal to zero or one. In contrast, in fuzzy set theory, it holds that $0 \leq \mu_{\hat{\xi}}(\xi) \leq 1$ which indicates a *degree* of membership. Hence $\mu_{\hat{\xi}}(\xi) = 0$ indicates no membership, while $\mu_{\hat{\xi}}(\xi) = 1$ means that ξ is fully included in $\hat{\xi}$. Furthermore, for each membership level α considered in the analysis and under the assumption of a convex membership function, there is an interval associated with the uncertain variable ξ. This interval associated with an α-level is represented by:

$$\xi_{\alpha}^{I} = \left\{ \xi \in \Xi : \mu_{\hat{\xi}}(\xi) \geq \alpha \right\}, \alpha \in (0, 1] \tag{4}$$

where ξ_{α}^{I} represents the possible set of values for an α-level of the membership function that ξ can adopt, and $(\cdot)^I$ denotes an interval. Note that this level corresponds to an interval defined by both its lower $\underline{\xi}_{\alpha}$ and upper $\bar{\xi}_{\alpha}$ bounds. From this definition it can be seen that a membership function corresponds to a collection of intervals indexed by a membership level. Membership functions can take different forms, such as trapezoidal functions and Gaussian curves, among others [36]. Because of their simplicity in construction, triangular-shaped functions are commonly used because of their wide applicability and advantages in the modeling process. Therefore, triangular membership functions are used in the present work. Fig. 1 illustrates a triangular membership function defined to characterize ξ. Note that the interval represented in Eq. (4) is shown in red in the figure. Additionally, note that only vertex information is required to construct the membership function of Fig. 1. It is noteworthy that, in practice, any number of fuzzy variables can be considered by simply repeating the definition of membership functions shown above.

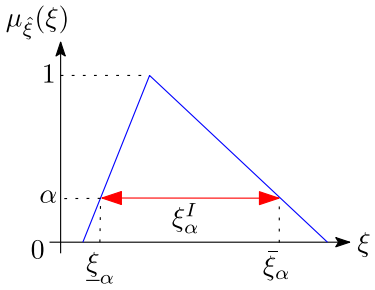

Fig. 1. Schematic representation of a fuzzy variable.

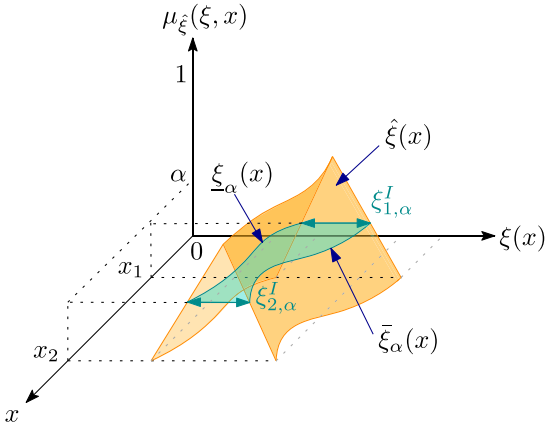

Fig. 2. Schematic diagram of fuzzy field.

2.3. Fuzzy fields

If the input parameters are spatially dependent, i.e. they are a function of the spatial coordinates in addition to being affected by uncertainty, fuzzy variable characterization cannot account for this dependence. One way to overcome this challenge is to use fuzzy fields [22]. Consider that only one input property ξ of the linear system of Eq. (1) exhibits spatial dependence. Therefore, the uncertainty in ξ depends on the spatial coordinate $\boldsymbol{x}$. This is denoted by $\xi(\boldsymbol{x})$, where $\boldsymbol{x}$ is contained in the domain Ω, which depends on the numerical model under consideration. To characterize this uncertainty, $\xi(\boldsymbol{x})$ can be described by means of a fuzzy field $\hat{\xi}(\boldsymbol{x})$. This fuzzy field is constructed using the information available at n_b control points, whose location within the domain Ω is denoted as $\boldsymbol{x}_j$, where $j = 1, \dots, n_b$. Therefore, defining the membership functions associated with the control points is a crucial step. To illustrate this, observe Fig. 2 which shows the case where ξ depends on a single spatial coordinate. It should be noted, though, that fuzzy fields can also be applied to multi-dimensional spatial dependencies. In the figure, it is possible to characterize the uncertain property ξ at two locations within the domain, x_1 and x_2, hence $n_b = 2$. At each of these locations, ξ can be characterized by a fuzzy variable $\hat{\xi}_j$, described by a membership function $\mu_{\hat{\xi}_j}(\xi_j)$, as presented in Section 2.2. Note also that for a given α-level of the membership functions, the interval $\xi_{1,\alpha}^I$ associated with the position x_1, and the interval $\xi_{2,\alpha}^I$ associated with the position x_2 are obtained. By using basis functions, the intervals associated with any position within the domain can be retrieved from the data available at the control points. The above implies that from the data contained in the intervals $\xi_{1,\alpha}^I$ and $\xi_{2,\alpha}^I$, the bounds of the uncertain parameter can be achieved at any position on the domain. Moreover, note that for this particular α-level, the fuzzy field is reduced to an interval field. This is represented by the interval field highlighted in Fig. 2.

The interval field associated with a given α-level $\xi_\alpha^I(\boldsymbol{x})$ corresponds to [37]:

$$\xi_\alpha^I(\boldsymbol{x}) = \sum_{j=1}^{n_b} \psi_j(\boldsymbol{x}, \boldsymbol{X}) \xi_{j,\alpha}^I \tag{5}$$

where $\boldsymbol{X}$ is a matrix containing the coordinates of the control points, i.e. $\boldsymbol{X} = [\boldsymbol{x}_1, \dots, \boldsymbol{x}_{n_b}]$, and $\xi_{j,\alpha}^I$ denotes the interval associated at the jth control point for the membership level α. $\psi_j(\cdot,\cdot)$ denotes the basis functions. It is noteworthy to point out that the basis functions are responsible for mapping the spatial uncertainty from the input domain to a reduced input space of n_b dimensions. Consequently, for a given α-level, the uncertainty in a space-dependent property $\xi(\boldsymbol{x})$ is reduced to that contained in the $\xi_{j,\alpha}^I$ intervals located at n_b control points, as shown in Eq. (5).

These basis functions are defined according to the following equation:

$$\psi_j(\boldsymbol{x}, \boldsymbol{X}) = \frac{w_j(\boldsymbol{x}, \boldsymbol{x}_j)}{\sum_{j_1=1}^{n_b} w_{j_1}(\boldsymbol{x}, \boldsymbol{x}_{j_1})}, \quad j = 1, \dots, n_b \tag{6}$$

where $w_j(\cdot,\cdot)$ is the weight function defined by:

$$w_j(\boldsymbol{x}, \boldsymbol{x}_j) = \frac{1}{\left(d(\boldsymbol{x}, \boldsymbol{x}_j)\right)^p} \tag{7}$$

where $d(\boldsymbol{x}, \boldsymbol{x}_j)$ is the considered distance measure between $\boldsymbol{x}$ and $\boldsymbol{x}_j$ and p is a positive real number. This parameter represents the influence that the information contained in the control point $\boldsymbol{x}_j$ is allowed to have on a given location $\boldsymbol{x}$ within the domain. In this paper, the value of p is considered equal to 2 [37]. Therefore, the weighting function used in this study corresponds to the Inverse Distance Weighting function introduced in [38].

From Eq. (5), it follows that the interval associated with any location $\boldsymbol{x}$ is expressed by the weighted sum of the intervals $\xi_{j,\alpha}^I$ at locations $\boldsymbol{x}_j$, where $j = 1, \dots, n_b$. Note that the weights assigned to each of the intervals described above are determined by their corresponding basis functions $\psi_j(\boldsymbol{x}, \boldsymbol{X})$, with $j = 1, \dots, n_b$, defined according to Eq. (6). Once an uncertain property is represented by a fuzzy field, the discrete representation of this property at each finite element must be determined to apply the finite element method. To project the uncertain property onto the model, this study considers the midpoint method [39]. Thus, the value of the uncertain property for a finite element can be completely described by the value at its centroid. The coordinate of a centroid is denoted by $\boldsymbol{x}_{C,q}$, with $q = 1, \dots, n_e$, where n_e is the number of elements in the model.

Therefore, the equation that represents the projection from the information held in the control points to the position of a given centroid $x_{C,q}$ is:

$$\xi_{C,q} = \sum_{j=1}^{n_b} \psi_j(\boldsymbol{x}_{C,q}, \boldsymbol{X}) \xi_j, \;\; \xi_j \in \xi_{j,\alpha}^I \tag{8}$$

where $\xi_{C,q}$ is the value of the uncertain parameter at the centroid of the element q. Note that for this purpose the basis functions ψ_j are evaluated at the centroid coordinates of the qth finite element.

2.4. Uncertainty propagation

When a system is modeled in the context of fuzzy analysis, the response r becomes a fuzzy variable $\hat{r}$ with an associated membership function, that is $\mu_{\hat{r}}(r)$. One way to determine $\mu_{\hat{r}}(r)$ is to resort the interpretation of a fuzzy variable as a collection of intervals indexed by a membership level, leading to the traditional α-level optimization strategy [23]. For this purpose, the membership function representing each uncertain parameter ξ is analyzed for discrete values of membership α_l, with $l = 1, \dots, n_c$, where n_c denotes the total number of discrete levels used. Note that in the case of the characterization by means

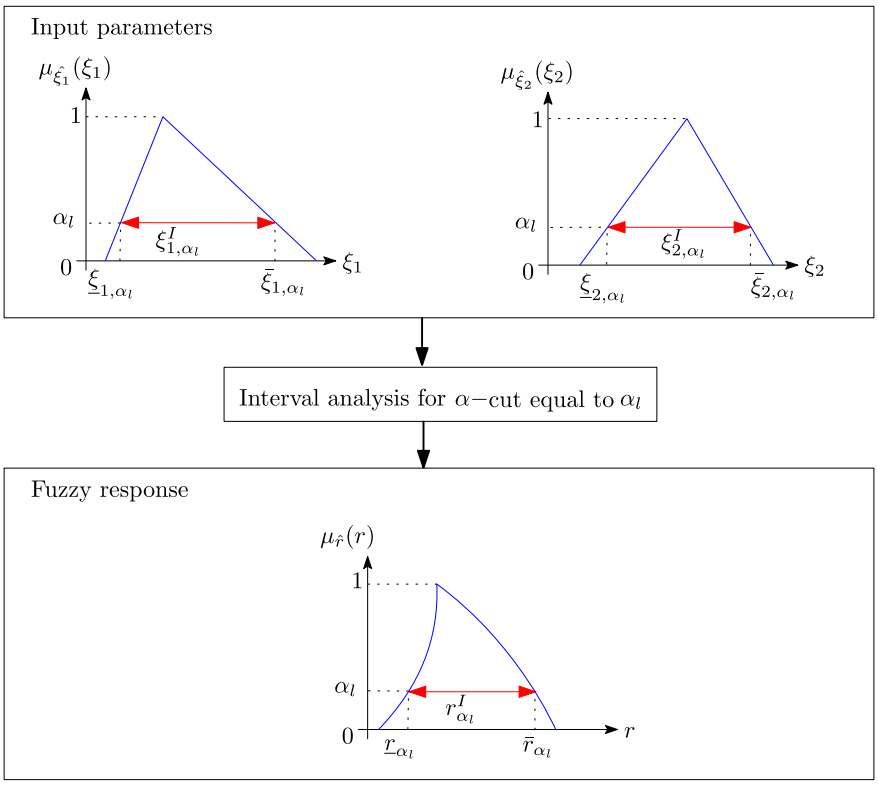

Fig. 3. α-level optimization process.

of fuzzy fields, the above also applies to the membership functions at each control point $\mu_{\hat{\xi}_j}(\xi_j)$. This is shown in Fig. 3, where the α-level optimization strategy is illustrated. Consider that the uncertain property ξ is characterized at two control points on the domain by the membership functions $\mu_{\hat{\xi}_1}(\xi_1)$ and $\mu_{\hat{\xi}_2}(\xi_2)$. Once the intervals for the level α_l are defined (ξ^I_{1,α_l}, ξ^I_{2,α_l} in the figure), an interval analysis is performed to estimate the bounds of the response. The interval obtained for the response at level α_l corresponds to $r^I_{\alpha_l}$, whose lower $\underline{r}_{\alpha_l}$ and upper $\bar{r}_{\alpha_l}$ bounds are obtained by solving the following optimization problems:

$$\underline{r}_{\alpha_l} = \min_{\xi \in \xi^I_{\alpha_l}} r(\xi) = \boldsymbol{\gamma}^T \boldsymbol{u}(\xi), \; l = 1, \ldots, n_c \tag{9}$$

$$\bar{r}_{\alpha_l} = \max_{\xi \in \xi^I_{\alpha_l}} r(\xi) = \boldsymbol{\gamma}^T \boldsymbol{u}(\xi), \; l = 1, \ldots, n_c \tag{10}$$

The intervals obtained for different membership levels α_l provide a discrete approximation to the membership function of the response. Nevertheless, solving the optimization problems for Eqs. (9) and (10) is not straightforward from a numerical viewpoint when the input parameters are characterized by fuzzy fields. Indeed, repeated deterministic analyses are required to find both bounds of the membership function of the response at a given α-level. This is because the optimization process evaluates different configurations of the input parameters within the intervals associated with the analyzed membership level until an extreme response is found. To settle these search intervals, the information of the fuzzy field must also be repeatedly mapped from the control points to the centroids of the finite elements. In addition, the result of the optimization scheme may be affected by local minima effects and be susceptible to numerical noise. Therefore, to achieve the characterization of the response of interest when considering fuzzy fields for modeling input properties, an efficient uncertainty propagation strategy must be employed. The approach used in this study is discussed in the following section.

3. Reduced-order model

3.1. General remarks

The previous subsection discussed the fuzzy field technique for incorporating uncertainty in input parameters into a finite element model. Once the uncertainty has been described by means of fuzzy fields, it is necessary to propagate it through the response, taking into account the spatial dependencies. The use of the α-level optimization scheme [23] mentioned above is one way to propagate the fuzzy uncertainty through a numerical model. Nevertheless, the implementation of this technique can be quite costly from a numerical point of view, as was discussed in Section 2.4. One way to overcome this obstacle is to use a surrogate model [25], such as a reduced-order model. This approximate model allows the equilibrium equations of the whole system to be projected onto a lower dimensional basis. This section details the formulation of the reduced-order model, taking into account the characterization of the input parameters by means of fuzzy fields.

3.2. Reduced-order model

Consider the linear system discussed in Section 2.1, which is represented by Eq. (1). This model depends on the uncertain parameters $\boldsymbol{\xi}$, which can be characterized using fuzzy variables and/or fuzzy fields. The response $\boldsymbol{u}(\xi)$ of this system is calculated approximately by projecting it into a reduced basis of dimension n_r. That is, the approximate response $\boldsymbol{u}^{\mathrm{A}}(\xi)$ is:

$$\boldsymbol{u}(\xi) \approx \boldsymbol{u}^{\mathrm{A}}(\xi) = \boldsymbol{\Phi}\boldsymbol{\beta}(\xi) \tag{11}$$

where $\boldsymbol{\Phi}$, is a basis, which is actually a matrix of dimension $n_d \times n_r$ whose columns are composed of the vectors $\boldsymbol{\phi}_i$, $i = 1, \ldots, n_r$; and $\boldsymbol{\beta}(\xi)$ is a vector of $n_r \times 1$ whose components depend on the uncertain parameters. The practical implementation of the approximation in Eq. (11) demands choosing an appropriate basis $\boldsymbol{\Phi}$ and calculating the vector $\boldsymbol{\beta}(\xi)$. Assuming that $\boldsymbol{\Phi}$ is already known, the vector $\boldsymbol{\beta}(\xi)$ is calculated by

means of a Galerkin method [40], which has been widely used in finite element analysis [41]. The formulation of the equilibrium equation (1) by the reduced basis $\boldsymbol{\Phi}$ using Galerkin's method (see [42] for more details) is equal to,

$$\boldsymbol{K}_R(\xi)\boldsymbol{\beta}(\xi) = \boldsymbol{f}_R(\xi) \tag{12}$$

where $\boldsymbol{K}_R(\xi)$ is the system's matrix of the reduced system, given by:

$$\boldsymbol{K}_R(\xi) = \boldsymbol{\Phi}^T \boldsymbol{K}(\xi)\boldsymbol{\Phi} \tag{13}$$

and $\boldsymbol{f}_R(\xi)$ is the reduced load vector,

$$\boldsymbol{f}_R(\xi) = \boldsymbol{\Phi}^T \boldsymbol{f}(\xi) \tag{14}$$

In these equations it is observed that the reduced system's matrix $\boldsymbol{K}_R(\xi)$ has dimension $n_r \times n_r$, while the reduced load vector $\boldsymbol{f}_R(\xi)$ has dimension n_r. Once the information of the system is projected onto the reduced basis, the problem narrows down to finding $\boldsymbol{\beta}(\xi)$ by solving Eq. (12). Note that this involves solving a linear system of n_r equations, which is quite favorable from a numerical point of view. This benefit is achieved because the dimension of the reduced-order model is smaller than that of the original system, i.e. $n_r \ll n_d$. Therefore, the approximate response r^{A} is:

$$r(\xi) \approx r^{\mathrm{A}}(\xi) = \boldsymbol{\gamma}^T \boldsymbol{\Phi}\boldsymbol{\beta}(\xi) \tag{15}$$

Once the expression for the response has been obtained from Eq. (15), an optimization algorithm can be applied, as discussed in the previous sections, to determine the membership function of the response. This procedure is described in detail in Section 3.5.

3.3. Construction of the reduced basis

As outlined earlier, it is of interest to characterize the model response using a reduced basis $\boldsymbol{\Phi}$. This basis enables the original system to be approximated with a reduced numerical cost. According to the literature, there are several techniques for constructing the reduced basis. One possibility is applying the snapshot method [26], which uses the information of complete simulations for a specific group of samples called key points. For this method, the choice of these key points is of utmost importance as it has a strong impact on the accuracy of the response. For example, selecting a very small number of these points can lead to inaccurate estimates of the response. Conversely, if the number of key points is too high, the basis will be large, reducing numerical efficiency. A more cost-effective numerical alternative is presented in [43], based on the optimization strategies discussed by [44]. More specifically, it is proposed to construct the reduced basis with information on the sensitivity of the response with respect to the uncertain parameters $\xi_j,\ j = 1, \ldots, n_\xi$ [43,44]. Therefore, the reduced basis $\boldsymbol{\Phi}$ is defined by:

$$\boldsymbol{\Phi} = \mathrm{orth}\left(\left[\boldsymbol{u}\left(\xi^0\right), \frac{\partial \boldsymbol{u}\left(\xi^0\right)}{\partial \xi_1}, \ldots, \frac{\partial \boldsymbol{u}\left(\xi^0\right)}{\partial \xi_{n_\xi}}\right]\right) \tag{16}$$

where orth $(\boldsymbol{X})$ denotes the ortho-normalization over the column space of $\boldsymbol{X}$, and the expansion point $\boldsymbol{\xi}^0$ is considered as a vector consisting of the uncertain parameter values associated with a membership equal to 1. $\boldsymbol{u}\left(\xi^0\right)$ corresponds to the system's response at the expansion point, and $\dfrac{\partial \boldsymbol{u}\left(\xi^0\right)}{\partial \xi_j}$ represents the jth derivative of the system's response at the expansion point with respect to the uncertain parameter ξ_j. The reduced basis allows one to perform a first-order Taylor expansion in the vicinity of ξ^0. Therefore, the reduced basis can capture the response of the system for small or moderate variations of the uncertain parameters. Since for the construction of the reduced basis only one exact analysis is required, the integration of sensitivity analysis into the basis construction process achieves a balance between computational efficiency and accuracy. The Appendix provides a detailed explanation of how the derivatives are calculated. In this work, the ortho-normalization process is performed using the Gram–Schmidt process. This method allows the ortho-normalization of a set of vectors in an inner Euclidean product space, which benefits the numerical stability of the reduced-order model [45]. The details of the ortho-normalization procedure are available in [43,46]. Numerical results reported there show that the procedure for calculating the reduced basis, as presented in Eq. (16), leads to accurate approximations of the system response. In cases where the reduced basis is not able to accurately approximate the response of the system, high-order terms can be included in the reduced basis formulation (see [46] for more details).

3.4. Error monitoring

The aforementioned formulation enables an approximate prediction of the response of the system which requires a lower numerical cost compared to the resolution of the original system. Nonetheless, the implementation of the reduced-order model only yields the response in an approximate way. Therefore, to obtain an accurate approximation of the response, it is necessary to monitor the error associated with $r^A(\xi)$.

The error produced by the reduced-order model $e(\xi)$ corresponds to:

$$e(\xi) = r(\xi) - r^A(\xi) \tag{17}$$

To determine $e(\xi)$, it would be necessary to know the value of the exact response $r(\xi)$, which, as discussed in Section 3, has a high numerical cost. To overcome this limitation, the calculation of the residual Euclidean norm associated with the equilibrium equation has been proposed in [46] as an alternative for measuring the error. This alternative error measure $\varepsilon(\xi)$ corresponds to,

$$\varepsilon(\xi) = \frac{\|\boldsymbol{K}(\xi)\boldsymbol{u}^A(\xi) - \boldsymbol{f}(\xi)\|}{\|\boldsymbol{f}(\xi)\|} \tag{18}$$

where $\|\cdot\|$ denotes the Euclidean norm. The calculation of $\varepsilon(\xi)$ represents an approximation of the real error associated with the application of the reduced-order model. Nonetheless, the results reported in the literature show that it provides a simple alternative to control that the error $e(\xi)$ does not overgrow [46,47].

3.5. Estimation of fuzzy response and basis enrichment

As discussed throughout this paper, it is of interest to estimate the membership function of the response $\mu_{\tilde{r}}(r)$ of a linear system under the influence of uncertain parameters characterized as fuzzy fields. The estimation of $\mu_{\tilde{r}}(r)$ can be performed by applying an optimization algorithm, as shown in Section 2.4, by giving solutions to Eqs. (9) and (10) for the discrete membership levels n_c under consideration. Note that if the objective function in these equations is modified by the expression derived to determine the approximate response of the system (see Eq. (15)), the problem reduces to,

$$\underline{r}^A_{\alpha_l} = \min_{\xi \in \xi^I_{\alpha_l}} r^A(\xi) = \boldsymbol{\gamma}^T \boldsymbol{\Phi}\boldsymbol{\beta}(\xi),\ l = 1, \ldots, n_c \tag{19}$$

$$\bar{r}^A_{\alpha_l} = \max_{\xi \in \xi^I_{\alpha_l}} r^A(\xi) = \boldsymbol{\gamma}^T \boldsymbol{\Phi}\boldsymbol{\beta}(\xi),\ l = 1, \ldots, n_c \tag{20}$$

where $\underline{r}^A_{\alpha_l}$ and $\bar{r}^A_{\alpha_l}$ are the approximate lower and upper bounds of the membership function of the response for a given α_l level, respectively. In this work, the Particle Swarm Optimization scheme [48] is used to compute the membership levels considered. Consequently, to find $\underline{r}^A_{\alpha_l}$ and $\bar{r}^A_{\alpha_l}$, it is necessary to evaluate the objective function repeatedly. This is because optimization algorithms, and in particular the Particle Swarm scheme, evaluate different candidates until the optimum is found. This process is illustrated in Fig. 4a for the first two α-cuts considered to discretely estimate the fuzzy response when $n_b = 2$. To approximate $\mu_{\tilde{r}}(r)$, the first task corresponds to the *initial step*. This corresponds to an exact analysis of the system at the expansion point

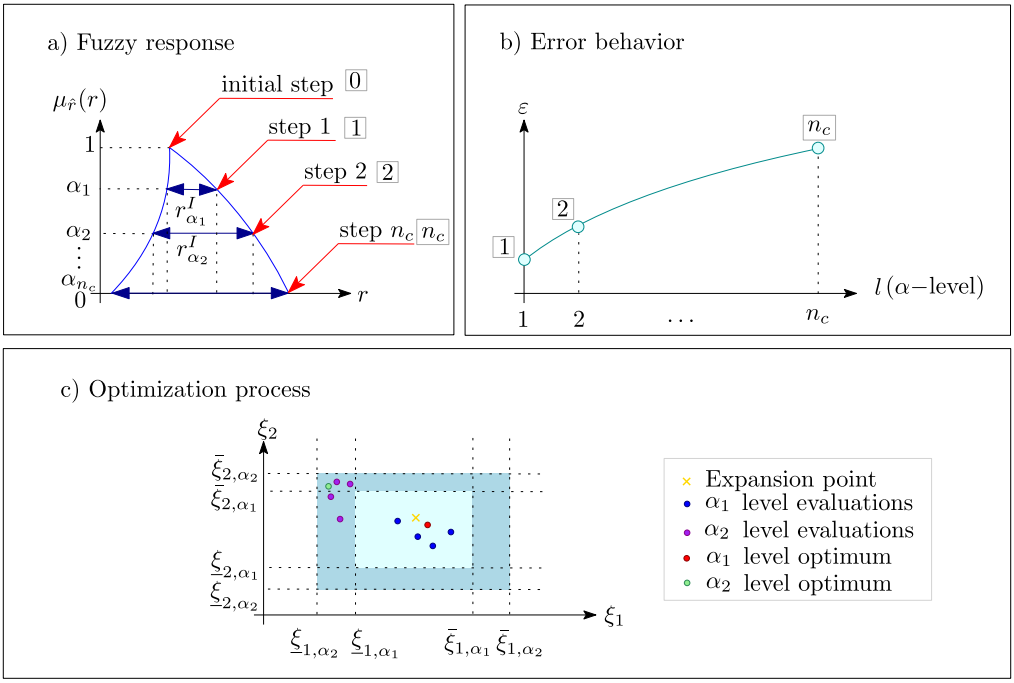

Fig. 4. Schematic representation of the error behavior. (*a*) Construction of the membership function of the response. (*b*) Error behavior. (*c*) Optimization procedure.

$\boldsymbol{\xi}^0$. This analysis allows the construction of the reduced basis $\boldsymbol{\Phi}$, as discussed in Section 3.3 and the Appendix. Once this step is completed, the optimization process is carried out for the membership levels α_1 and α_2, in the *step 1* and *step 2*, respectively. It should be noted that since the level α_1 is close to 1, the approximate response is expected to be quite close to the exact one. This is because all the possible values explored during the optimization phase will be relatively close to the expansion point. This is illustrated in Fig. 4c where the search space for the level α_1 is shown in light blue. Note that the expansion point, shown in yellow, is close to all the evaluations performed by the algorithm (blue circles in the figure) and close to the optimum (red circle). Conversely, for *step 2*, whose search space is larger than that for level α_1, the quality of the approximation is expected to decrease, since such a search space may contain values far from $\boldsymbol{\xi}^0$. Therefore, the evaluations performed by the search algorithm (indicated by purple circles) and the optimum (green circle) may be far from the expansion point.

The above behavior results in a significant increase in error when trying to find the optimum for membership levels close to 0. This is depicted schematically in Fig. 4b, which illustrates the maximum error as a function of the membership level l, $l = 1, \ldots, n_c$. In this context, the *maximum error* is understood as the maximum between the values of ε (see Eq. (18)) evaluated at the bounds for the current membership level l (that is, minimum and maximum of the response of interest for the current membership under analysis). It is expected that the error will continue to grow for the rest of the α-cuts. This behavior does not provide any control over the increase of the error ε. In fact, the reduced-order model, as formulated, does not provide any feedback on the error that it introduces. In other words, the basis of the reduced model is static with respect to ε. This approach is not ideal as it can lead to significant errors indicating an inaccurate approximation. Therefore, there is a problem with the accumulation of errors as different levels of α_l are examined. In order to avoid a significant decrease in the accuracy of the approximation when analyzing membership levels closer to 0, a strategy proposed in [46] is implemented. The proposed strategy is illustrated in Fig. 5 for the case of $n_c = 2$. First, a threshold error ε_t is defined, which corresponds to the maximum error $\varepsilon(\boldsymbol{\xi})$ accepted between the exact and approximate models. This threshold is represented by the orange segmented line in Fig. 5b. Then, for the extrema of the response found at each membership level, the error ε is calculated according to Eq. (18). Note that, in Fig. 5b, for the α_1 level, the maximum error obtained between the two bounds, $\underline{r}^A_{\alpha_1}$ and $\bar{r}^A_{\alpha_1}$, is less than the defined threshold. Nonetheless, in the case of α_2, one of the optimal parameter sets (for the lower or upper bound) produces an error that exceeds the considered threshold. This means that the realization of the uncertain parameters that produces an error greater than the tolerance $\boldsymbol{\xi}^*$, can be associated with either the lower or the upper bound. When this happens, the following three actions are taken:

1. An exact analysis is carried out. This means that Eq. (1) is solved to obtain $\boldsymbol{u}\left(\boldsymbol{\xi}^*\right)$. This allows one to obtain $r\left(\boldsymbol{\xi}^*\right)$ *exactly*.
2. The reduced basis $\boldsymbol{\Phi}$ is updated, enriching it with the information given by $\boldsymbol{u}\left(\boldsymbol{\xi}^*\right)$.
3. Both bounds are recalculated with the new reduced basis.

The second point described above is illustrated in Fig. 5c, where $\boldsymbol{\Phi}_0$ represents the reduced basis obtained in the *initial step*. $\boldsymbol{\Phi}_0$ was used to determine the bounds of the membership function of the response for the levels α_1 and α_2, before updating the basis. In the figure, the column of the reduced basis representing the response is plotted in light blue, while the components associated with the partial derivatives with respect to the information of the uncertain parameters are plotted in orange. After detecting that one of the bounds associated with the level α_2 exceeds the threshold, an additional analysis is performed. This yields a new, updated reduced basis $\boldsymbol{\Phi}_1$ containing an additional column shown in pink in Fig. 5c. The response associated with the exact analysis $\boldsymbol{u}\left(\boldsymbol{\xi}^*\right)$ is included in the reduced basis $\boldsymbol{\Phi}_1$ as a column vector by means of the Gram–Schmidt process. From a mathematical viewpoint, the reduced basis $\boldsymbol{\Phi}_1$ is given by:

$$\boldsymbol{\Phi}_1 = \left[\boldsymbol{\Phi}_0, \frac{\boldsymbol{v}\left(\boldsymbol{\xi}^*\right)}{\|\boldsymbol{v}\left(\boldsymbol{\xi}^*\right)\|}\right] \tag{21}$$

where $\boldsymbol{v}\left(\boldsymbol{\xi}^*\right)$ corresponds to:

$$\boldsymbol{v}\left(\boldsymbol{\xi}^*\right) = \boldsymbol{u}\left(\boldsymbol{\xi}^*\right) - \boldsymbol{\Phi}_0\left(\boldsymbol{\Phi}_0^T \boldsymbol{u}\left(\boldsymbol{\xi}^*\right)\right) \tag{22}$$

Therefore, when determining the new optimums for the α_2 level, it will be possible to keep the error below ε_t. It is noteworthy that

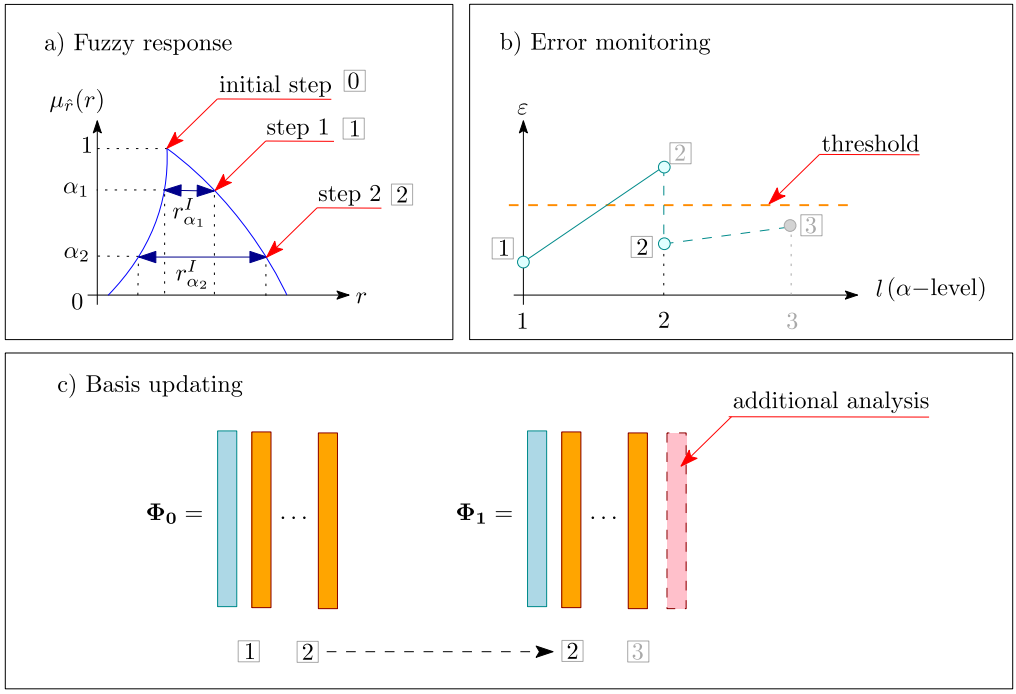

Fig. 5. Schematic of the basis updating procedure. (*a*) Construction of the membership function of the response. (*b*) Error monitoring. (*c*) Basis updating procedure.

the previous discussion assumes that, for a given level, only one of the bounds exceeds the threshold. Nevertheless, it is possible that both bounds exceed the considered threshold. In this case, the update step can be repeated, enriching the basis with the information of the other limit. Thus, there are two possible cases when determining the extrema of the response of the membership function at this level: (1) it is not necessary to re-enrich the basis, or (2) an additional basis update is required. In the first case, the optimum search continues until it is successful, i.e., $\underline{r}^A_{\alpha_2}$ and $\bar{r}^A_{\alpha_2}$ are found. Then, it proceeds to analyze the next level (e.g., level α_3, as shown in Fig. 5b). In the second case, the basis is enriched, and both extrema of the response are determined again, that is, Eqs. (19) and (20) are solved again. Moreover, note that for this α_3 level, both situations described above could happen. Fig. 5b shows the first scenario. Consequently, the proposed strategy ensures that the error produced by the reduced-order model remains below the threshold at the identified extrema of the response for a given α-level membership value. The maximum admissible error considered in this study is $\varepsilon_t = 10^{-4}$, according to the recommendations in [47]. Therefore, the convergence of the procedure is guaranteed with the proposed strategy. At worst, the reduced basis is expanded until it includes n_d vectors (n_d being the total number of degrees of freedom of the problem). At this stage, any response of the system can be exactly captured by the reduced basis, which no longer needs to be expanded.

3.6. Summary of the proposed strategy

The proposed methodology for performing a fuzzy field analysis considering a reduced-order model for uncertainty propagation can be summarized in the following steps, which are also illustrated in Fig. 6.

1. Define the numerical model and the response of interest r (Eq. (3)).
2. Identify the parameters of the model that are uncertain.
3. Define the uncertainty in the parameters by means of a fuzzy field $\hat{\xi}(\boldsymbol{x})$.
   (a) Set the number n_b and the position $\boldsymbol{x}_j$, with $j = 1, \dots, n_b$, of the control points according to the information available.
   (b) At each control point, characterize the uncertain parameters using membership functions $\mu_{\hat{\xi}_j}(\xi_j)$.
4. Set up the finite element mesh associated with the model. For each element, retrieve its centroid $x_{C,q}$.
5. Select a number of n_c α-cuts and define the membership values α_l, with $l = 1, \dots, n_c$.
6. Select an error threshold ε_t.
7. Identify the expansion point $\boldsymbol{\xi}^0$. Solve Eq. (1) for $\boldsymbol{\xi}^0$ to calculate $\boldsymbol{u}(\boldsymbol{\xi}^0)$.
8. Perform a sensitivity analysis for $\boldsymbol{u}(\boldsymbol{\xi}^0)$ (see Appendix) to construct the reduced basis $\boldsymbol{\Phi}$ applying Eq. (16).
9. Set $l = 1$. Solve both optimization problems in Eqs. (19) and (20).
   (a) Calculate the approximate response r^A solving Eqs. (12) and (15).
   (b) Compute the error measure ε with Eq. (18) for the identified minimum and maximum values of the response at the corresponding membership level.
   (c) Check the error behavior for the minimum value of the response identified in step 9.b. If $\varepsilon < \varepsilon_t$, go to step 9.e. Otherwise, calculate the exact response by solving Eqs. (1) and (3). For this purpose, use the information of the realization $\boldsymbol{\xi}^*$ (associated to the minimum) that produces an error greater than the tolerance.
   (d) Enrich the reduced basis $\boldsymbol{\Phi}$ using the Gram–Schmidt method outlined in Eqs. (21) and (22), with the information of $\boldsymbol{u}(\boldsymbol{\xi}^*)$. Return to step 9.a.
   (e) Check the error behavior for the maximum value of the response identified in 9.b. If $\varepsilon < \varepsilon_t$, go to step 10. Otherwise, calculate the exact response by solving Eqs. (1) and (3). For this purpose, use the information of the realization $\boldsymbol{\xi}^*$ (associated to the maximum) that produces an error greater than the tolerance.
   (f) Enrich the reduced basis $\boldsymbol{\Phi}$ using the Gram–Schmidt method outlined in Eqs. (21) and (22), with the information of $\boldsymbol{u}(\boldsymbol{\xi}^*)$. Return to step 9.a.

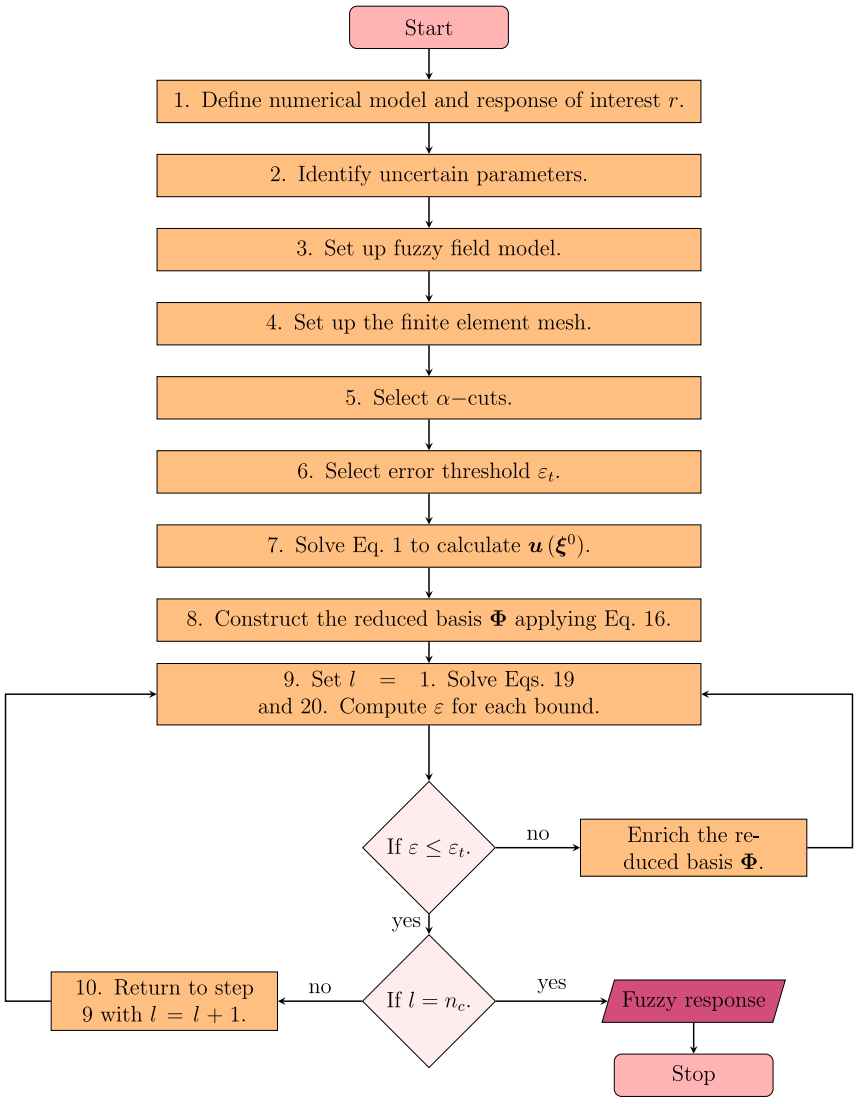

Fig. 6. Flowchart of fuzzy field analysis with reduced-order model.

10. Set $l = l + 1$. If $l = n_c$, stop the process. Otherwise, return to step 9 with $l = l + 1$.

4. Illustrative examples

4.1. Heat transfer on by-product concrete block

Fig. 7 shows the first problem studied which corresponds to the heat flow in a concrete block made with recycled (by-products) materials. With the ongoing need to minimize energy consumption in the design of sustainable buildings, proper evaluation of the thermal performance of building envelope components is a strict requirement. Therefore, there is a need for proper characterization of the thermal properties of, for example, by-product concrete blocks [49]. However, when by-products are used, the thermal conductivity in the material may behave in-homogeneously as the medium becomes more porous under the addition of sawdust, lime sludge, and other recycled materials [50]. One way to capture the spatial uncertainty of this property is to use fuzzy fields. Therefore, the objective of this study is to determine the variation in the total heat flow through the block. The thermal conductivity is assumed to be isotropic and with the available (scarce) information, it is possible to construct membership functions at three control points. At each of these positions, the thermal conductivity value was characterized by a membership function, which allowed the uncertainty of this property to be represented by a fuzzy field. The membership functions associated with the control points are shown in Fig. 8. For the construction of these membership functions, it should be noted that samples, expert knowledge, and information from previous studies, among others, can be used. The thermal conductivity values defined in this study were based on literature reports [50]. Regarding the edge temperatures, the temperature of the inner side of the concrete block was considered deterministic and equal to 25 [°C] (298.15 [K]). In contrast, the temperature of the outside of the block was considered uncertain and was characterized by a fuzzy variable with the membership function of Fig. 9.

For the finite elements of the numerical model, triangular quadratic elements were considered, with each element represented by its centroid. A total of 10854 nodes and 5428 elements were considered to represent the concrete block. The matrix of thermal conductivity of each element was calculated by numerical integration, considering three integration points. After determining the internal temperature of the block, the heat flow rate was calculated with respect to the unit width of the block. To obtain the total heat flow, the sum of the flow over all boundary nodes at the bottom side of the concrete block was calculated. For more details on the calculation of the total flow, see e.g. [13,27]. 10 α-levels were considered to obtain the membership function representing the flow response in discrete form. The values

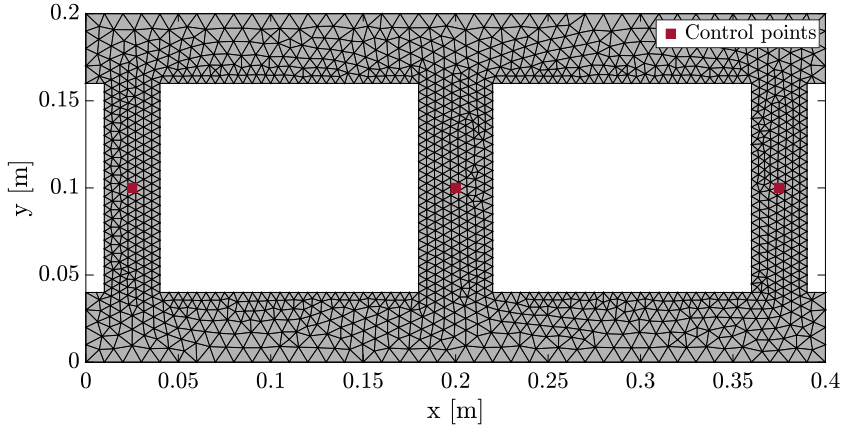

Fig. 7. Finite element mesh and control point locations for heat problem.

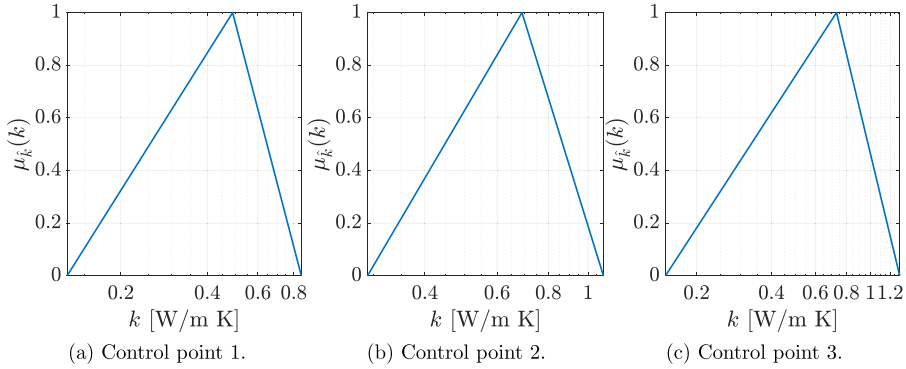

Fig. 8. Membership function of thermal conductivity at control points. From left to right the control points are located at: (a) $x = 0.025$ [m], $y = 0.100$ [m]. (b) $x = 0.200$ [m], $y = 0.100$ [m]. (c) $x = 0.375$ [m], $y = 0.100$ [m].

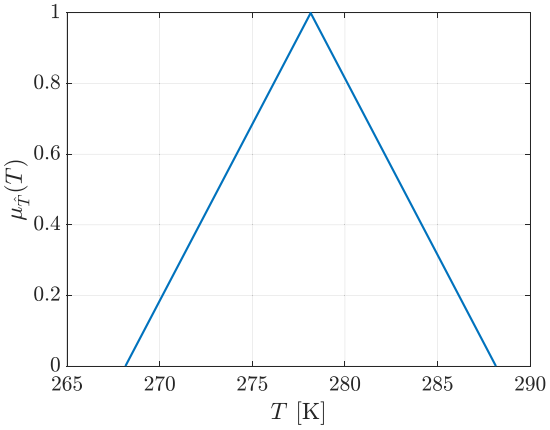

Fig. 9. Membership function of top side boundary temperature of the concrete block.

associated with the lower and upper bounds of the fuzzy heat flow response for the 10 levels studied were determined using the Particle Swarm Optimization scheme. The concrete block was studied considering two models: the exact system and the approximate model. The results were evaluated considering that (a) there is no basis updating process ($\varepsilon_t \to \infty$) and (b) there is a basis updating process with a threshold of $\varepsilon_t = 10^{-6}$.

4.1.1. Solution without basis updating

The fuzzy response obtained for the total heat flow on the inner side of the concrete block is shown in Fig. 10, where this flow is denoted as r. Initially, it was assumed that there is no basis updating procedure, i.e., $\varepsilon_t \to \infty$. From Fig. 10 it is observed that the membership function associated with the resolution of the exact system (blue curve) and the membership function associated with the reduced model (orange curve) are identical. A non-linear relationship between the uncertain input parameters and the response associated with the membership level has been identified by the shape of the membership function obtained. This behavior is more pronounced on the left side of the membership function. Since the thermal conductivity is characterized by a fuzzy field, the total flow response is also fuzzy, as explained earlier in this paper. Therefore, it is necessary to analyze the heat flow response according to the membership level considered. This gives an indication of the degree of uncertainty associated with this response. For example, if level $\alpha_l = 0.5$ is analyzed, the heat flow response can take any value in the interval [7.67, 26.26] [W/m^2] per m. Nonetheless, the value obtained for the deterministic analysis at $\mu_{\tilde{r}}(r) = 1$ was equal to 15.62 [W/m^2]. With such results, users can develop an overall understanding of the effect of uncertainty in the input parameters, and the relationship between the sensitivity of the response and the level of membership under consideration. In terms of computational cost, the solution of the reduced-order model was 268 times faster than that of the original system, demonstrating the computational advantage of using the reduced-order model without compromising accuracy.

In addition, for comparison with traditional methods, note that the results are also computed taking into account the Vertex Method [51]. When the response of the deterministic system varies monotonically with respect to the uncertain parameters, the Vertex Method ensures an exact result for optimizing the interval problem defined in Eq. (9) and (10). As shown in Fig. 10, the results for the Vertex Method for this example are identical to the solution using the exact system and the reduced-order model. Nonetheless, it requires $2^{n_\xi} = 16$ exact

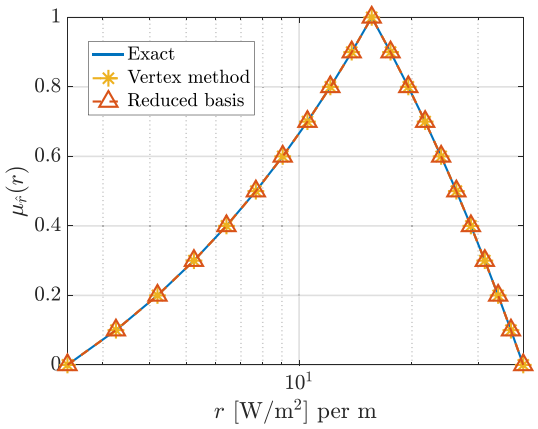

Fig. 10. Membership function of the total heat flow response in the concrete block, considering $\epsilon_t = \infty$.

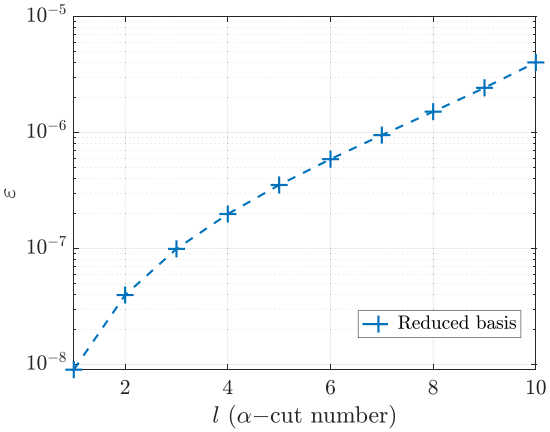

Fig. 11. Error behavior considering $\epsilon_t = \infty$ for the total heat flow response in the concrete block.

analysis (for each membership level) to obtain the membership function of the response, which is much higher compared to the requirements considering the reduced-order model (see Table 2).

Fig. 11 shows the error behavior when finding the optimum associated with different membership levels for approximate total heat flow response. The increasing behavior of the error observed in the figure shows that there is a loss of precision in the search for the optima that are associated with membership levels close to 0. This is explained by the fact that for levels closer to membership 0, these optima may be far from the expansion point used to construct the reduced basis. Nevertheless, the error associated with the reduced basis was below 10^{-5} for all the membership levels analyzed.

4.1.2. Solution with basis updating

In this case, the threshold level was chosen such that $\epsilon_t = 10^{-6}$. Such value was chosen as it is more stringent than the suggested value of 10^{-4} (see Section 3.4). The membership function obtained for the response of the total heat flow r is shown in Fig. 12. Note that in this case the results are also compared to the Vertex Method (see Table 2). In terms of error performance, Fig. 13 shows how the error is maintained below the established threshold for all estimated membership levels. The comparison between the maximum error committed by the reduced-order model for the case with and without the basis updating procedure is shown in the Table 1. To better understand the error behavior, note that Fig. 14 shows the number of additional analyses performed to identify the bounds of the fuzzy response for each level

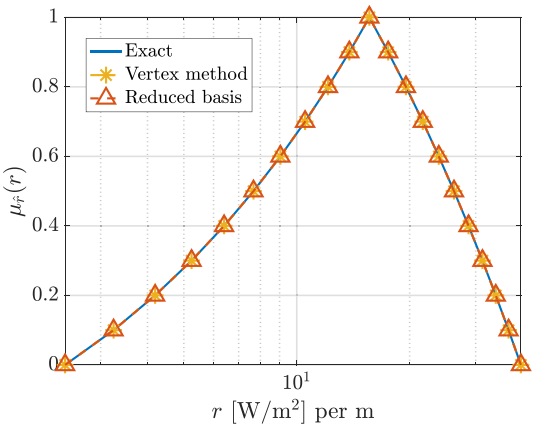

Fig. 12. Membership function of the total heat flow response in the concrete block, considering $\epsilon_t = 10^{-6}$.

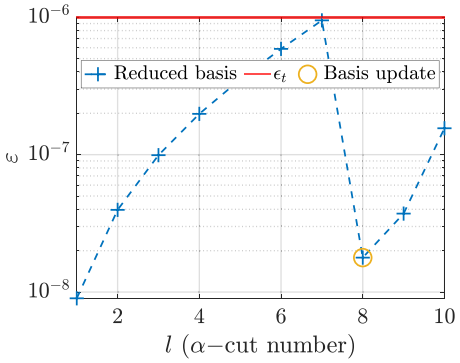

Fig. 13. Error behavior considering $\epsilon_t = 10^{-6}$ for the total heat flow response in the concrete block.

Table 1
Maximum error associated with the reduced-order model for the total heat flow response in the concrete block.

Without basis updating	With basis updating
4.0208×10^{-6}	9.4951×10^{-7}

α_l. Note that it was not necessary to enrich the reduced basis for the first seven levels. This is because, although the error increased, it remained below the set threshold. Nevertheless, in the case of level α_8, it was necessary to update the basis once. This results in a decrease of the error obtained for this level in Fig. 13.

Regarding the computational time, a speed-up of 239 was obtained comparing the resolution of the reduced-order model with the exact system. This decrease in speed-up compared to the result obtained for the case shown in the previous section is explained by the additional exact analysis that had to be performed to enrich the reduced basis.

Since the errors made by the reduced-order model without updating the basis and with its application are quite small for this simple example (see Table 1), the heat flow response was computed considering fewer columns of the reduced basis to demonstrate the effect of introducing the updating strategy. Note how in Fig. 15, the membership function (in purple) obtained considering the alternative reduced basis overestimates the bounds of the heat flow response for the different membership levels analyzed. Moreover, observe that this overestimation is more pronounced for the levels approaching zero. The aforementioned behavior produces that the error associated with the alternative basis (see Fig. 16) is higher than the one obtained by the reduced-order model considering the full reduced basis (see Fig. 11) for the different membership levels computed. As a result, two additional analyses are

Table 2
Number of exact analyses performed to compute the total heat flow response.

Method	Number of exact analysis
α-level optimization exact model	422
α-level optimization ROM model, without basis updating	1
α-level optimization ROM model, with basis updating	2
Vertex Method	160

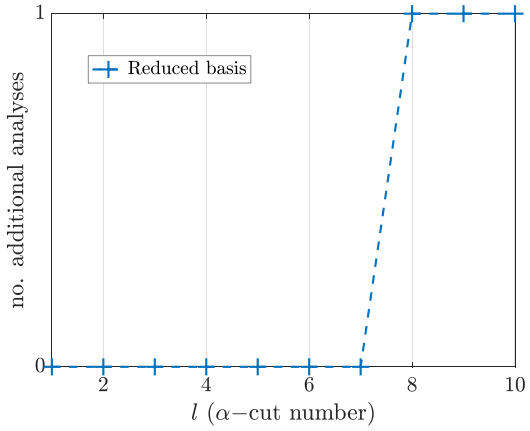

Fig. 14. Number of additional analyses considering $\epsilon_t = 10^{-6}$ for the total heat flow response in the concrete block.

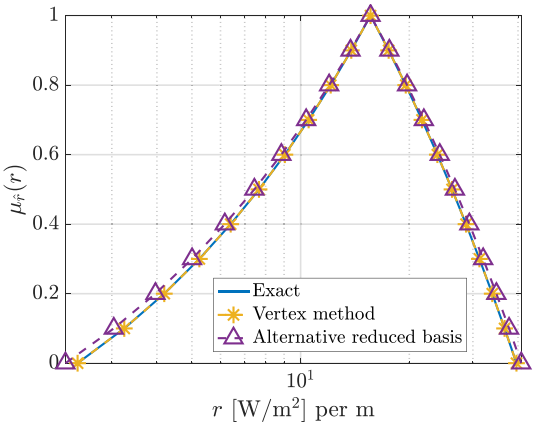

Fig. 15. Membership function of the total heat flow response in the concrete block, considering $\epsilon_t = \infty$ for the alternative reduced basis.

required to keep the error below the threshold (see Figs. 18 and 19) when using the basis updating approach to compute the heat flow response shown in Fig. 17. Note that the maximum error of the approximate model has now decreased by about two orders of magnitude when the basis updating strategy is taken into account (see Table 3). In contrast, the results shown in Table 1, which do not include the alternative reduced basis, show a lower benefit in terms of error, due to the quality of the reduced-order model. These results not only highlight the accuracy advantage of the method at a minimal numerical cost (requiring only two additional exact analyses) but also demonstrate that for a simple model such as this one, it is possible to obtain satisfactory results with a reduced basis that includes only a subset of the columns containing the sensitivity information. This, in conjunction with the basis updating procedure, yields results comparable to those obtained when considering the full basis with updating (see Tables 1 and 3). In terms of speed-up, the resolution of the approximate model with the alternative reduced basis was 191 and 255 times faster than the exact model, with and without basis updating, respectively.

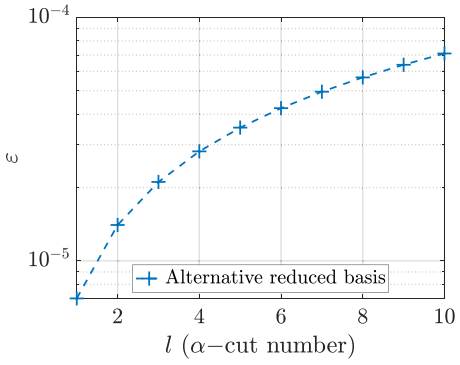

Fig. 16. Error behavior considering $\epsilon_t = \infty$ (alternative reduced basis) for the total heat flow response in the concrete block.

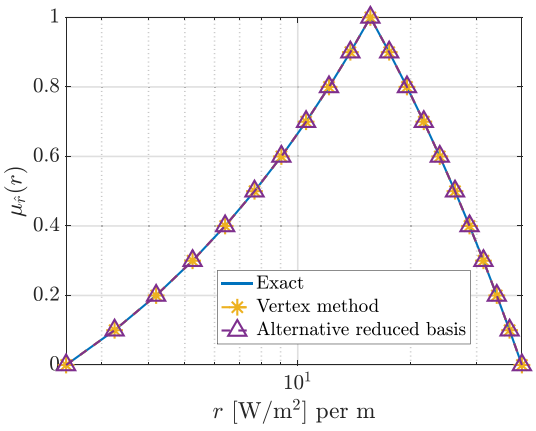

Fig. 17. Membership function of the total heat flow response in the concrete block, considering $\epsilon_t = 10^{-6}$ for the alternative reduced basis.

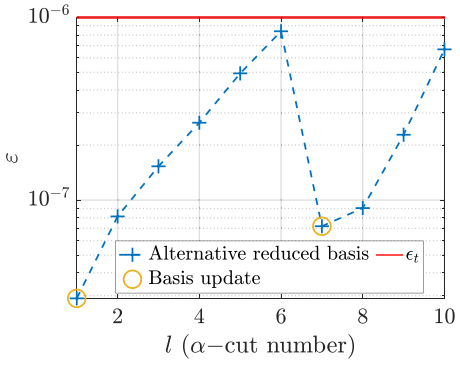

Fig. 18. Error behavior considering $\epsilon_t = 10^{-6}$ (alternative reduced basis) for the total heat flow response in the concrete block.

4.2. Seepage under impervious dam

The proposed methodology is also applied to the analysis of saturated steady-state seepage flow through a porous medium under an

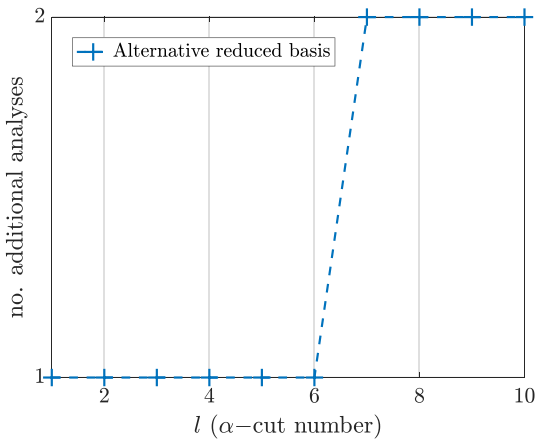

Fig. 19. Number of additional analyses considering $\varepsilon_t = 10^{-6}$ (alternative reduced basis) for the total heat flow response in the concrete block.

Table 3
Maximum error associated with the reduced-order model (alternative reduced basis) for the total heat flow response in the concrete block.

Without basis updating	With basis updating
7.1073×10^{-5}	8.3887×10^{-7}

impervious dam. The dam is founded on a permeable soil layer 20 [m] deep, bounded by an impermeable rock layer. The dam has an extent of 20 [m], as shown in Fig. 20. A water column of deterministic height $h = 10$ [m] is retained upstream of the dam. The flow rate at the dam outlet is a crucial result of the seepage analysis for design purposes. The seepage flow rate was calculated in terms of the unit width of the dam after determining the piezometric head associated with the model [27]. The sum of the flow over all the boundary nodes on the left side of the dam was calculated to obtain the total flow [13].

It is considered that the horizontal k_H and vertical k_V hydraulic conductivities of the soil layer are uncertain due to effects such as the spatial variation of the soil [52], as well as the inaccuracy and sparseness of the field measurements [53]. Therefore, the horizontal k_H and vertical k_V conductivities were characterized using fuzzy fields. Four control points are considered where the dependence between the two conductivities is included considering $0.1k_H \leq k_V \leq k_H$ [54,55]. The membership functions associated with each control point are shown in Fig. 21. For the construction of these membership functions, typical values reported in the literature are considered (see [56]).

A finite element model with 3183 nodes and 1498 quadratic triangular elements was considered to study the seepage problem. Each element has 6 degrees of freedom. Ten α-levels were used to estimate the response membership function, i.e., $n_c = 10$. The hydraulic conductivity matrix of each element was calculated using numerical integration, considering three integration points. It should be noted that the flow rate is also uncertain due to the characterization of the parameters described above. Therefore, the main objective of this study was to determine the membership function representing the flow uncertainty $\hat{r}$ downstream of the dam. To estimate the above membership levels, the Particle Swarm Optimization scheme [48] was used to determine the exact and approximate response. The dam was studied by considering an exact system and an approximate model. The results were evaluated considering that (a) there is no basis updating process ($\varepsilon_t \to \infty$) and (b) there is a basis updating process with a threshold of $\varepsilon_t = 10^{-4}$.

4.2.1. Solution without basis updating

The membership function obtained for the response of the total flow downstream of the dam is shown in Fig. 22, where this flow is denoted as r. The error threshold was considered as $\varepsilon_t \to \infty$, i.e., the system was studied without considering the enrichment of the reduced basis $\boldsymbol{\Phi}$. The membership function of the approximate response and the exact model are very similar. Some minimal discrepancies are observed on the left-hand side of the membership function for low membership values. Similar to the concrete block analysis, the fuzzy response of the total flow must be analyzed in terms of the associated membership level. For example, if level $\alpha_l = 0.5$ is investigated, the total flow at the dam exit can take any value in the interval $[8.12 \times 10^{-6}, 2.47 \times 10^{-5}]$ [m^3/s] per [m]. Whereas, for the deterministic case (i.e., $\mu_{\hat{r}}(r) = 1$), the total flow was equal to 1.60×10^{-5} [m^3/s] per [m]. In this example, the system response was also calculated using the Vertex Method. Despite the precision of the Vertex Method in providing an accurate response, it is important to recognize the significant number of exact analyses that are required. This is due to the number of uncertain parameters involved in this example, which are related to the number of control points considered and the anisotropy of the soil properties. As a result, the computational cost of obtaining the system's response using the Vertex Method is significantly higher than the cost of implementing the proposed strategy (see Table 5), which highlights the benefit of the proposed strategy. Comparing this result with the one achieved for the concrete block problem in terms of the range of the interval obtained, the range is rather large, which is due to the large uncertainty associated with the hydraulic conductivity of the soil. In terms of computation time, a speed-up of 58 was obtained for the approximate model compared to the solution of the exact model. The reason for the smaller numerical gain compared to the heat problem is that the hydraulic conductivity of the soil is assumed to be anisotropic, while the thermal conductivity of the recycled concrete block is assumed to be isotropic, which implies that a larger number of terms n_k is involved in the representation of the system's matrix (see Eq. (2)). In addition, the number of uncertain parameters is higher in this case due to the larger number of control points considered in the definition of the fuzzy field. As a result, the reduced basis is larger, which slows down the speed-up.

On the other hand, Fig. 23 shows the evolution of the maximum error ε in each α-cut of the membership function associated with the flow at the dam downstream. An increasing error behavior was observed as a function of the membership level analyzed, being higher in the case of levels closer to zero. This behavior had indeed been anticipated. When examining membership levels that approach zero, this leads to a notably expanded search space within the optimization process. As a result, the optimal solution might end up being more distant from the expansion point, as was discussed in Section 3.4.

4.2.2. Solution with basis updating

The membership function obtained for the flow response downstream of the dam, considering $\varepsilon_t = 10^{-4}$, is shown in Fig. 24. In this case, the implementation of the proposed methodology has been studied considering the updating of reduced basis $\boldsymbol{\Phi}$. The membership function of the approximate response and the exact model are practically identical. The differences on the left-hand side for low values of the membership function obtained in the previous case are not observed when the basis updating strategy is carried out.

Concerning the error behavior, Fig. 25 shows how the error remains below the established threshold for all estimated membership levels. A comparison of the maximum error produced by the reduced-order model for the case with and without the basis updating procedure is shown in Table 4. To understand the error behavior, note that Fig. 26 shows the number of additional analyses performed to determine the bounds of the fuzzy response for each level α_l. Note that for the first three levels, α_1, α_2, and α_3, it was not necessary to enrich the reduced basis. The reason for this is that even though there was an increase in the error, it was below the threshold value. Nonetheless, in the case of level α_4, it was necessary to update the basis once. This leads to a decrease in the error obtained for this level in Fig. 25. Note that the observed behavior of the error is expected. After updating the reduced

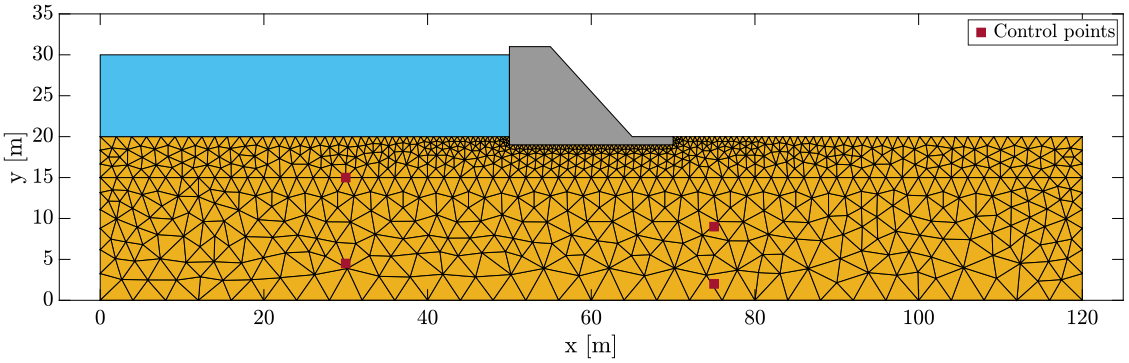

Fig. 20. Finite element mesh and control point locations for seepage problem.

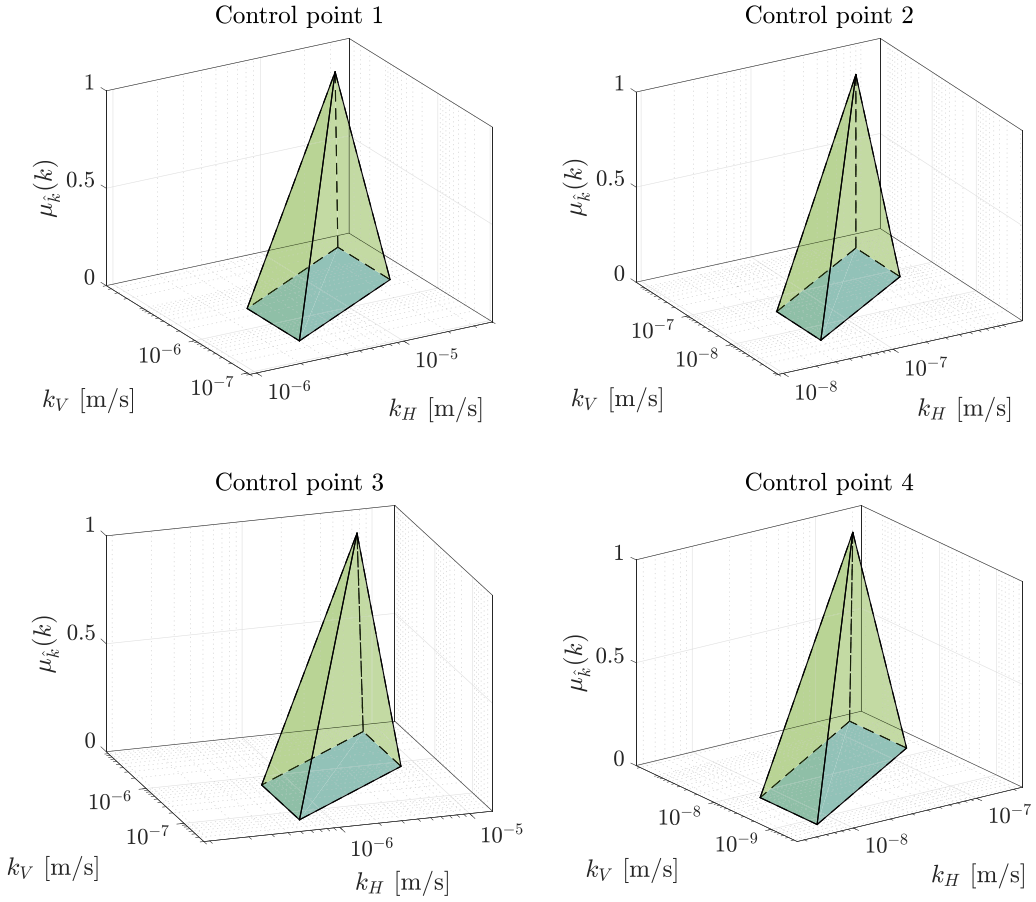

Fig. 21. Membership function of hydraulic conductivities at control points. Each control point is located at (1) $x = 30$ [m], $y = 15$ [m]. (2) $x = 30$ [m], $y = 4.5$ [m]. (3) $x = 75$ [m], $y = 9$ [m]. (4) $x = 75$ [m], $y = 2$ [m].

basis, as shown in Fig. 5b, one should notice a decrease in the error measure for the newly computed bounds of the level that exceeds the threshold. Subsequently, this measure is expected to increase again when the bounds of the subsequent α-level are determined. Thus, the increasing trend of the error from levels α_1 to α_3 should have been maintained for level α_4, but since the error measure for this level exceeded the defined tolerance, the basis was enriched. Consequently, it is due to this enrichment that the error reported in Fig. 25 for level α_4 is lower compared to the previous level. Due to the continued increase in error from level α_4 to α_7, a new additional analysis was required to determine the limits of level α_8.

Finally, another additional analysis was required for the membership level α_{10}, resulting in a total of 3 additional analyses during the entire optimization process, which are highlighted in Fig. 25. Regarding the computation times, a speed-up of 43 was obtained. The decrease in terms of speed-up is due to the three additional exact analyses required to enrich the reduced basis, compared with the analysis considering $\varepsilon_t \to \infty$.

5. Summary and conclusions

This paper presents an efficient technique to estimate the fuzzy response of linear systems considering the spatial uncertainty in the input

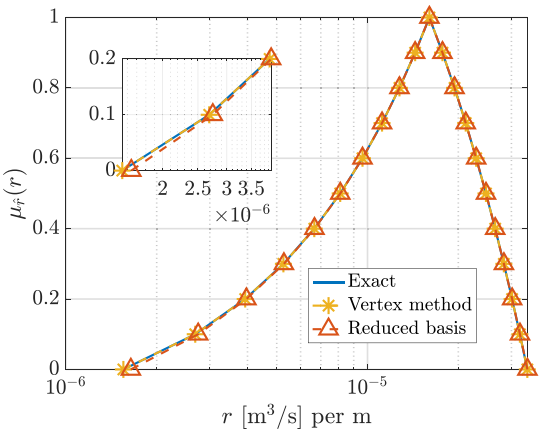

Fig. 22. Membership function of the flow response downstream of the dam, considering $\epsilon_t = \infty$.

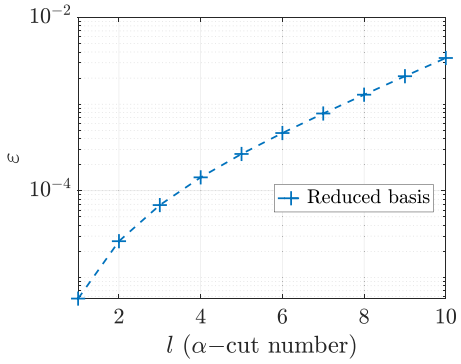

Fig. 23. Error behavior considering $\epsilon_t = \infty$ for the flow response downstream of the dam.

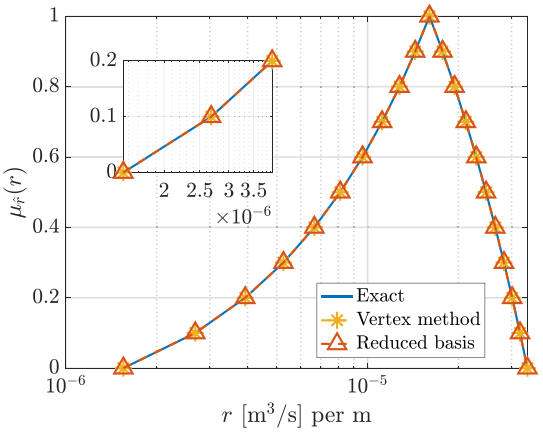

Fig. 24. Membership function of the flow response downstream of the dam, considering $\epsilon_t = 10^{-4}$.

Table 4
Maximum error associated with the reduced-order model for the flow response downstream of the dam.

Without basis updating	With basis updating
3.4120×10^{-3}	9.7523×10^{-5}

properties by applying a reduced-order model. The approach is formulated to propagate the uncertain properties characterized by fuzzy

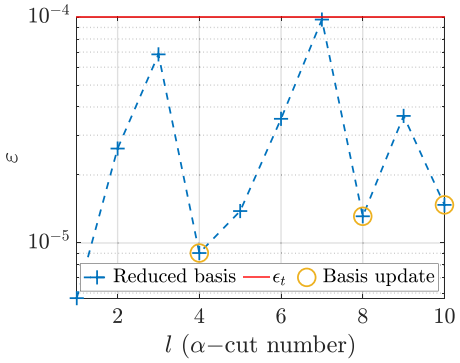

Fig. 25. Error behavior considering $\epsilon_t = 10^{-4}$ for the flow response downstream of the dam.

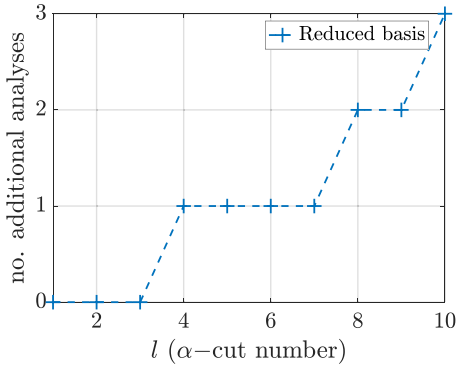

Fig. 26. Number of additional analyses performed to obtain the flow response downstream of the dam, considering $\epsilon_t = 10^{-4}$.

fields through an optimization scheme. In particular, two challenges have been addressed, as discussed in detail below.

First, the spatial dependencies in uncertain parameters with scarce available data have been taken into account following a non-probabilistic approach. By requiring only the membership functions at control points, fuzzy fields facilitate the characterization of uncertain input parameters under problems such as lack, scarcity, and incompleteness of data. This is because these membership functions require a minimum amount of information for their definition (vertex information) and allow the incorporation of expert knowledge. Additionally, users can define the location and number of control points according to the available data to account for spatial dependencies. This enables design analysis to be performed even with limited uncertain information is available. An additional benefit of extending interval field analysis to the fuzzy framework is the inclusion of sensitivity analysis. Beyond the best- and worst-case scenario analysis that can be obtained from interval analysis, the fuzzy component allows users to evaluate different cases and get feedback on the characterization of their uncertain parameters. Therefore, fuzzy analysis is a suitable alternative to traditional probabilistic methods under severe uncertainty.

The second challenge addressed in this proposal is related to the numerical cost of characterizing uncertain parameters using fuzzy fields. To avoid the numerical cost of projecting the fuzzy field into the FEM associated with each search of the fuzzy response optima, a reduced-order model has been applied. The reduced-order model is formulated to require only a single exact analysis of the system and its respective sensitivities. To overcome accuracy problems, the reduced basis is enriched adaptively to ensure the quality of the approximation. For this purpose, the error associated with the reduced-order model was examined.

Table 5
Number of exact analyses performed to compute the flow response downstream of the dam.

Method	Number of exact analysis
α-level optimization exact model	486
α-level optimization ROM model, without basis updating	1
α-level optimization ROM model, with basis updating	4
Vertex Method	2560

The reduced-order model was tested in the study of steady-state heat flow in a concrete block made of recycled materials and in steady-state saturated seepage under a dam. The results show that an accurate estimation of the fuzzy responses can be obtained with reduced numerical effort while controlling the quality of the results. The above was evidenced by the high performance observed in the reduced-order model and, in particular, its coupling with the application of fuzzy fields to propagate uncertainty to the response. In the case of the by-product concrete block study, only one additional analysis was required, while in the case of the dam problem, three additional analyses were performed.

It is noteworthy that the application of fuzzy field analysis coupled with a reduced-order model introduces certain limitations in the interpretability of results when compared to probability-based approaches. Unlike probability-based methods that provide a full probabilistic description of the response of interest and assess the failure probability of the system, fuzzy field analysis provides interval estimates of the response at a particular membership value. These estimates provide insight into the degree of uncertainty and help identify, for example, worst-case scenarios. Therefore, while fuzzy fields are valuable in the presence of limited data, researchers should carefully consider the purpose of the study when choosing this approach.

Future research efforts will be directed towards exploring more complex systems. This includes the exploration of dynamic systems, further types of responses, and the expansion into larger physical dimensions. Similarly, the use of fuzzy fields to characterize other types of uncertain parameters, such as those related to geometry, will be explored. Finally, in the case of anisotropic properties such as soil hydraulic conductivity, it is suggested to explore alternative strategies for incorporating dependency structures at and between control points. For example, one approach could be to incorporate the decomposition of bi-variate admissible sets as presented in [57,58].

CRediT authorship contribution statement

Nataly A. Manque: Writing – original draft, Visualization, Validation, Software, Methodology, Investigation, Formal analysis, Conceptualization. **Marcos A. Valdebenito:** Writing – review & editing, Validation, Supervision, Investigation, Formal analysis, Conceptualization. **Pierre Beaurepaire:** Writing – review & editing, Supervision, Formal analysis, Conceptualization. **David Moens:** Writing – review & editing, Validation, Formal analysis. **Matthias G.R. Faes:** Writing – review & editing, Validation, Supervision, Investigation, Formal analysis, Conceptualization.

Declaration of competing interest

The authors declare that they have no known competing financial interests or personal relationships that could have appeared to influence the work reported in this paper.

Data availability

Data will be made available on request.

Appendix. Derivatives for reduced basis

Replacing the parametric expression of the system's matrix (see Eq. (2)) in the equilibrium equation (1), it follows that:

$$\left(\boldsymbol{K}_0 + \sum_{k=1}^{n_\xi} \boldsymbol{K}_k \xi_k\right) \boldsymbol{u}(\boldsymbol{\xi}) = \boldsymbol{f}(\boldsymbol{\xi}) \tag{A.1}$$

$$\boldsymbol{K}_0 \boldsymbol{u}(\boldsymbol{\xi}) + \sum_{k=1}^{n_\xi} \boldsymbol{K}_k \xi_k \boldsymbol{u}(\boldsymbol{\xi}) = \boldsymbol{f}(\boldsymbol{\xi}) \tag{A.2}$$

From where, the jth derivative with respect to ξ_j, applying the direct method described in [59], corresponds to:

$$\left(\boldsymbol{K}_0 + \sum_{j=1}^{n_\xi} \boldsymbol{K}_j \xi_j\right) \frac{\partial \boldsymbol{u}(\boldsymbol{\xi})}{\partial \xi_j} + \sum_{j=1}^{n_\xi} \boldsymbol{K}_j \boldsymbol{u}(\boldsymbol{\xi}) = \frac{\partial \boldsymbol{f}(\boldsymbol{\xi})}{\partial \xi_j} \tag{A.3}$$

Replacing the left-hand term with the relationship of Eq. (2) for the system's matrix:

$$\boldsymbol{K}(\boldsymbol{\xi}) \frac{\partial \boldsymbol{u}(\boldsymbol{\xi})}{\partial \xi_j} = \frac{\partial \boldsymbol{f}(\boldsymbol{\xi})}{\partial \xi_j} - \sum_{j=1}^{n_\xi} \boldsymbol{K}_j \boldsymbol{u}(\boldsymbol{\xi}) \tag{A.4}$$

Finally, taking apart the partial derivative of the displacement it is obtained that:

$$\frac{\partial \boldsymbol{u}(\boldsymbol{\xi})}{\partial \xi_j} = \boldsymbol{K}^{-1}(\boldsymbol{\xi}) \left(\frac{\partial \boldsymbol{f}(\boldsymbol{\xi})}{\partial \xi_j} - \sum_{j=1}^{n_\xi} \boldsymbol{K}_j \boldsymbol{u}(\boldsymbol{\xi}) \right) \tag{A.5}$$

References

[1] Diodato N. Spatial uncertainty modeling of climate processes for extreme hydro-geomorphological events hazard monitoring. J Environ Eng 2006;132(11):1530–8. http://dx.doi.org/10.1061/(asce)0733-9372(2006)132:11(1530).

[2] Shafei B, Alipour A. Estimation of corrosion initiation time in reinforced concrete bridge columns: How to incorporate spatial and temporal uncertainties. J Eng Mech 2015;141(10). http://dx.doi.org/10.1061/(asce)em.1943-7889.0000861.

[3] Phillips DL, Marks DG. Spatial uncertainty analysis: propagation of interpolation errors in spatially distributed models. Ecol Model 1996;91(1–3):213–29. http://dx.doi.org/10.1016/0304-3800(95)00191-3.

[4] Vanmarcke E. Random fields, analysis and synthesis. MIT Press; 1983.

[5] Beer M, Zhang Y, Quek ST, Phoon KK. Reliability analysis with scarce information: Comparing alternative approaches in a geotechnical engineering context. Struct Saf 2013;41:1–10. http://dx.doi.org/10.1016/j.strusafe.2012.10.003.

[6] Faes M, Moens D. Recent trends in the modeling and quantification of non-probabilistic uncertainty. Arch Comput Methods Eng 2019;27(3):633–71. http://dx.doi.org/10.1007/s11831-019-09327-x.

[7] Faes MG, Broggi M, Chen G, Phoon K-K, Beer M. Distribution-free p-box processes based on translation theory: Definition and simulation. Probab Eng Mech 2022;69:103287. http://dx.doi.org/10.1016/j.probengmech.2022.103287.

[8] Schietzold FN, Schmidt A, Dannert MM, Fau A, Fleury RMN, Graf W, et al. Development of fuzzy probability based random fields for the numerical structural design. GAMM-Mitt 2019;42(1):e201900004. http://dx.doi.org/10.1002/gamm.201900004.

[9] Faes M, Broggi M, Patelli E, Govers Y, Mottershead J, Beer M, et al. A multivariate interval approach for inverse uncertainty quantification with limited experimental data. Mech Syst Signal Process 2019;118:534–48. http://dx.doi.org/10.1016/j.ymssp.2018.08.050.

[10] Möller B, Beer M. Fuzzy randomness. Springer Berlin Heidelberg; 2004, http://dx.doi.org/10.1007/978-3-662-07358-2.

[11] Zhang D, Shu L, Li S. Fuzzy structural element method for solving fuzzy dual medium seepage model in reservoir. Soft Comput 2020;24(21):16097–110. http://dx.doi.org/10.1007/s00500-020-04926-4.

[12] Faes MG, Daub M, Marelli S, Patelli E, Beer M. Engineering analysis with probability boxes: A review on computational methods. Struct Saf 2021;93:102092. http://dx.doi.org/10.1016/j.strusafe.2021.102092.

[13] Degrauwe D, Lombaert G, Roeck GD. Improving interval analysis in finite element calculations by means of affine arithmetic. Comput Struct 2010;88(3–4):247–54. http://dx.doi.org/10.1016/j.compstruc.2009.11.003.

[14] Sofi A, Romeo E. A novel interval finite element method based on the improved interval analysis. Comput Methods Appl Mech Engrg 2016;311:671–97. http://dx.doi.org/10.1016/j.cma.2016.09.009, URL http://www.sciencedirect.com/science/article/pii/S004578251631129X.

[15] Sofi A, Romeo E, Barrera O, Cocks A. An interval finite element method for the analysis of structures with spatially varying uncertainties. Adv Eng Softw 2019;128:1–19. http://dx.doi.org/10.1016/j.advengsoft.2018.11.001.

[16] Callens RR, Faess MG, Moens D. Multilevel quasi-Monte Carlo for interval analysis. Int J Uncertain Quantif 2022;12(4):1–19. http://dx.doi.org/10.1615/int.j.uncertaintyquantification.2022039245.

[17] Dang C, Wei P, Faes MG, Valdebenito MA, Beer M. Interval uncertainty propagation by a parallel bayesian global optimization method. Appl Math Model 2022;108:220–35. http://dx.doi.org/10.1016/j.apm.2022.03.031.

[18] Faes M, Moens D. Identification and quantification of spatial interval uncertainty in numerical models. Comput Struct 2017;192:16–33. http://dx.doi.org/10.1016/j.compstruc.2017.07.006, URL http://www.sciencedirect.com/science/article/pii/S0045794917303802.

[19] van Mierlo C, Faes MG, Moens D. Inhomogeneous interval fields based on scaled inverse distance weighting interpolation. Comput Methods Appl Mech Engrg 2021;373:113542. http://dx.doi.org/10.1016/j.cma.2020.113542.

[20] Callens RR, Faes MG, Moens D. Local explicit interval fields for non-stationary uncertainty modelling in finite element models. Comput Methods Appl Mech Engrg 2021;379:113735. http://dx.doi.org/10.1016/j.cma.2021.113735.

[21] Verhaeghe W, De Munck M, Desmet W, Vandepitte D, Moens D. A fuzzy finite element analysis technique for structural static analysis based on interval fields. In: Proceedings of the 4th international workshop on reliable engineering computing. Singapore: Research Publishing Services; 2010, p. 117–28.

[22] Verhaeghe W, Desmet W, Vandepitte D, Joris I, Seuntjens P, Moens D. Application of interval fields for uncertainty modeling in a geohydrological case. In: Computational methods in stochastic dynamics. Springer Netherlands; 2013, p. 131–47. http://dx.doi.org/10.1007/978-94-007-5134-7_8.

[23] Möller B, Graf W, Beer M. Fuzzy structural analysis using α-level optimization. Comput Mech 2000;26(6):547–65.

[24] Hanss M. Applied fuzzy arithmetic. Springer Berlin Heidelberg; 2005, http://dx.doi.org/10.1007/b138914.

[25] Sudret B, Marelli S, Wiart J. Surrogate models for uncertainty quantification: An overview. In: 2017 11th European conference on antennas and propagation. IEEE; 2017, http://dx.doi.org/10.23919/eucap.2017.7928679.

[26] Gogu C, Passieux J-C. Efficient surrogate construction by combining response surface methodology and reduced order modeling. Struct Multidiscip Optim 2013;47(6):821–37. http://dx.doi.org/10.1007/s00158-012-0859-4.

[27] Valdebenito MA, Hernández HB, Jensen HA. Probability sensitivity estimation of linear stochastic finite element models applying line sampling. Struct Saf 2019;81:101868. http://dx.doi.org/10.1016/j.strusafe.2019.06.002.

[28] Gram JP, Schmidt E. On the application of the theory of orthogonal functions to the solution of problems in linear algebra: Part i. Z Math Phys 1902;47:269–77.

[29] Lewis RW, Morgan K, Thomas HR, Seetharamu KN. Finite element method in heat transfer. John Wiley & Sons; 1996.

[30] Lu J, Li J, Song Z, Zhang W, Yan C. Uncertainty and sensitivity analysis of heat transfer in hypersonic three-dimensional shock waves/turbulent boundary layer interaction flows. Aerosp Sci Technol 2022;123:107447. http://dx.doi.org/10.1016/j.ast.2022.107447.

[31] Forster M, Seibold F, Krille T, Waidmann C, Weigand B, Poser R. A Monte Carlo approach to evaluate the local measurement uncertainty in transient heat transfer experiments using liquid crystal thermography. Measurement 2022;190:110648. http://dx.doi.org/10.1016/j.measurement.2021.110648.

[32] Griffiths D, Fenton G. Seepage beneath water retaining structures founded on spatially random soil. Geotechnique 1993;43(4):577–87.

[33] Zadeh L. Fuzzy sets, information and control. 1965.

[34] Beer M, Ferson S, Kreinovich V. Imprecise probabilities in engineering analyses. Mech Syst Signal Process 2013;37(1–2):4–29. http://dx.doi.org/10.1016/j.ymssp.2013.01.024.

[35] Moens D, Vandepitte D. Fuzzy finite element method for frequency response function analysis of uncertain structures. AIAA J 2002;40(1):126–36. http://dx.doi.org/10.2514/2.1621.

[36] Mitaim S, Kosko B. What is the best shape for a fuzzy set in function approximation?. In: Proceedings of IEEE 5th international fuzzy systems. IEEE; 1996, http://dx.doi.org/10.1109/fuzzy.1996.552354.

[37] Faes M, Moens D. Identification and quantification of spatial interval uncertainty in numerical models. Comput Struct 2017;192:16–33. http://dx.doi.org/10.1016/j.compstruc.2017.07.006, URL http://www.sciencedirect.com/science/article/pii/S0045794917303802.

[38] Shepard D. A two-dimensional interpolation function for irregularly-spaced data. In: Proceedings of the 1968 23rd ACM national conference. 1968, p. 517–24.

[39] Der Kiureghian A, Ke J-B. The stochastic finite element method in structural reliability. Probab Eng Mech 1988;3(2):83–91.

[40] Deb MK, Babuška IM, Oden J. Solution of stochastic partial differential equations using galerkin finite element techniques. Comput Methods Appl Mech Engrg 2001;190(48):6359–72. http://dx.doi.org/10.1016/s0045-7825(01)00237-7.

[41] Zienkiewicz OC. The finite element method. Butterworth-Heinemann; 2000.

[42] Boyaval S, Le Bris C, Maday Y, Nguyen N, Patera A. A reduced basis approach for variational problems with stochastic parameters: Application to heat conduction with variable Robin coefficient. Comput Methods Appl Mech Engrg 2009;198(41):3187–206. http://dx.doi.org/10.1016/j.cma.2009.05.019, URL http://www.sciencedirect.com/science/article/pii/S0045782509002114.

[43] González I, Valdebenito M, Correa J, Jensen H. Calculation of second order statistics of uncertain linear systems applying reduced order models. Reliab Eng Syst Saf 1832;190(2019):106514. http://dx.doi.org/10.1016/j.ress.2019.106514, URL http://www.sciencedirect.com/science/article/pii/S0951832019301115, com/science/article/pii/S095.

[44] Noor A, Lowder H. Approximate techniques of structural reanalysis. Comput Struct 1974;4(4):801–12. http://dx.doi.org/10.1016/0045-7949(74)90046-7.

[45] Gautschi W. Numerical analysis. 2nd ed. Birkhäuser Boston; 2012, http://dx.doi.org/10.1007/978-0-8176-8259-0.

[46] Valdebenito M, Jensen H, Wei P, Beer M, Beck A. Application of a reduced order model for fuzzy analysis of linear static systems. ASCE-ASME J Risk Uncertain Eng Syst B Mech Eng 2021;7(2):020904. http://dx.doi.org/10.1115/1.4050159, arXiv:https://asmedigitalcollection.asme.org/risk/article-pdf/7/2/020904/6687872/risk_007_02_020904.pdf.

[47] Gogu C, Chaudhuri A, Bes C. How adaptively constructed reduced order models can benefit sampling-based methods for reliability analyses. Int J Reliab Qual Saf Eng 2016;23(05):1650019. http://dx.doi.org/10.1142/S0218539316500194.

[48] Kennedy J, Eberhart R. Particle swarm optimization. In: Proceedings of ICNN'95-international conference on neural networks, vol. 4. Perth, WA, Australia: IEEE; 1995, p. 1942–8.

[49] Ganjian E, Jalull G, Sadeghi-Pouya H. Using waste materials and by-products to produce concrete paving blocks. Constr Build Mater 2015;77:270–5. http://dx.doi.org/10.1016/j.conbuildmat.2014.12.048.

[50] Blanco JM, Frómeta YG, Madrid M, Cuadrado J. Thermal performance assessment of walls made of three types of sustainable concrete blocks by means of FEM and validated through an extensive measurement campaign. Sustainability 2021;13(1):386. http://dx.doi.org/10.3390/su13010386.

[51] Dong W, Shah HC. Vertex method for computing functions of fuzzy variables. Fuzzy Sets and Systems 1987;24(1):65–78. http://dx.doi.org/10.1016/0165-0114(87)90114-x.

[52] Baroni G, Zink M, Kumar R, Samaniego L, Attinger S. Effects of uncertainty in soil properties on simulated hydrological states and fluxes at different spatio-temporal scales. Hydrol Earth Syst Sci 2017;21(5):2301–20. http://dx.doi.org/10.5194/hess-21-2301-2017.

[53] Guan Z, Wang Y. CPT-based probabilistic liquefaction assessment considering soil spatial variability, interpolation uncertainty and model uncertainty. Comput Geotech 2022;141:104504. http://dx.doi.org/10.1016/j.compgeo.2021.104504.

[54] Fanchi JR. 4- porosity and permeability. In: Fanchi JR, editor. Integrated reservoir asset management. Boston: Gulf Professional Publishing; 2010, p. 49–69. http://dx.doi.org/10.1016/B978-0-12-382088-4.00004-9, URL https://www.sciencedirect.com/science/article/pii/B9780123820884000049.

[55] Shedid SA. Vertical-horizontal permeability correlations using coring data. Egypt J Petrol 2019;28(1):97–101. http://dx.doi.org/10.1016/j.ejpe.2018.12.007.

[56] Elhakim AF. Estimation of soil permeability. Alex Eng J 2016;55(3):2631–8. http://dx.doi.org/10.1016/j.aej.2016.07.034.

[57] Faes M, Moens D. Multivariate dependent interval finite element analysis via convex hull pair constructions and the extended transformation method. Comput Methods Appl Mech Engrg 2019;347:85–102. http://dx.doi.org/10.1016/j.cma.2018.12.021.

[58] Faes M, Moens D. On auto- and cross-interdependence in interval field finite element analysis. Internat J Numer Methods Engrg 2020;121(9):2033–50. http://dx.doi.org/10.1002/nme.6297.

[59] Haftka R, Gürdal Z. Elements of structural optimization. 3rd ed. Dordrecht, The Netherlands: Kluwer; 1992.